A Summary of the Thesis entitled

"Syntheses, Molecular Structures, Spectroscopic Characterization and Bio-mimetic Activity of Vanadium Complexes"

To be Submitted

As a partial fulfilment for the award of the degree of

DOCTOR OF PHILOSOPHY

In

Chemistry

By

Ms. Neetu Patel

Under the supervision of

Prof. A. K. Prajapati

Department of Chemistry

Faculty of Science

Maharaja Sayajirao University of Baroda

Vadodara 390 002

India

April 2021

Summary of the Thesis work

To be submitted to The Maharaja Sayajirao University of Baroda for the award of the degree of DOCTOR OF PHILOSOPHY in Chemistry.

Name of Student: Neetu Patel

Title of the Thesis: "Syntheses, Molecular Structures, Spectroscopic Characterization and Bio-mimetic Activity of Vanadium Complexes"

Name of the Supervisor: Prof. A. K. Prajapati
The Maharaja Sayajirao University of Baroda

Faculty: Faculty of Science, The Maharaja Sayajirao University of Baroda.

Department: Department of Chemistry

Registration No.: FOS/2115

Date of Registration: 28th August, 2018

Neetu Patel
Research Student

Prof. A. K. Prajapati
Research Guide

The Thesis work is presented in form of the following chapters:

Chapter 1

Introduction

Chapter 2

Metal-organic hybrids based on a $[VO_2(L)]$-tecton with cations of imidazole derivatives: Synthesis, characterization and *in vitro* antidiabetic activity

Chapter 3

New oxidovanadium(IV/V) complexes with tridentate Schiff base ligands: Synthesis, molecular structure and *in vitro* antidiabetic activity

Chapter 4

Anionic dioxidovanadium(V) complexes $[VO_2(L)]^-$ with (Z)-N'-(2-hydroxy-3-methoxybenzylidene)isonicotinichydrazide as proligand and cation of imidazole units as ancillary ligands: Synthesis, characterization and *in-vitro* antidiabetic activity

Chapter 5

Syntheses, spectral characterization and antidiabetic activities of vanadium(IV/V) complexes with bi-and tridentate ligands (In situ reaction)

Chapter 1: Introduction

Vanadium (Z = 23) is a transition element and placed in the fourth row in the periodic table with electronic configuration $[Ar]3d^3 4s^2$. It was discovered in 1801 by Del Rio's and rediscovered severally in 1831 by Swedish Chemist Nils Gabriel Sefstrom. Sefstrom named this element vanadium after the Scandinavian goddess Vanadis. It is widely distributed in nature and forms up to 0.02 % of the earth's crust with 60 ores. Vanadium metal is hard and steel-grey metal with two naturally occurring isotopes namely ^{51}V (99.76 %) and ^{50}V (0.24 %). It is mostly used in the steel industry as an additive. Its compounds are useful and used as catalysts, in ceramics, pigments, batteries and industries. This element has got nuclear applications, as rust-resistant elements, in manufacturing superconductive magnets along with within manufacturing of high-speed steel and iron made tools.

Vanadium exists in several oxidation states *viz.*, -1, 0, +2, +3, +4 and +5. Vanadium pentoxide (V_2O_5) is the most common and working form of vanadium. Other commonly used vanadium salts are ammonium metavanadate (NH_4VO_3), sodium metavanadate ($NaVO_3$) and sodium orthovanadate (Na_3VO_4). The toxicity of vanadium is popular and its toxicity differs significantly due to the compound's nature. Vanadium pentoxide is the most toxic and mobile form [1].

Vanadium is an essential element in biological systems. Vanadium is mainly complexed *in vivo*. It easily couples with proteins like transferrin, albumin, haemoglobin and glutathione [2]. It is also nutritionally essential in mammals, but its specific biological role in human is not much explored. The required quantity of vanadium is ca. 100-200 µg [3]. This element is equally useful for the growth and development of goats, rats, mice and chicks [4]. The use of vanadium in humans was suggested in the case of pathological states such as malnutrition, anaemia, tuberculosis and diabetes. It is tested that the diabetic patients prescribed sodium metavanadate excreted less glucose in urine [5].

The inhibition of catalyst activity is thought to be one amongst the effective methods for the treatment of diabetes. Inorganic vanadate complexes have been proposed to have potential in the inhibition of α-glucosidase [6], α-amylase [7] and glucose-6-phosphate [8]. It has been found that athletes took vanadium sulphate as a supplement at doses up to 60 mg/day to increase the weight during training. The toxicity of vanadium compounds is low due to quick excretion in urine [9]. Although the commercial applications of inorganic compounds are limited due to their poor absorption and fast excretion in the gastrointestinal tract in the human body [10, 11]. Therefore, inorganic chemists shifted their research views to the organic vanadium complexes that have higher absorptive capacity than inorganic vanadium. Encouraging complexes to consist of neutral $V^{IV}O$ species with bidentate anionic ligand (L^-) with composition VOL_2; for example $[VO^{IV}(maltato)_2]$ (BMOV) and $[VO^{IV}(Etmaltato)_2]$ (BEOV).

BMOV is a benchmark complex for the new molecules with antidiabetic feature [12, 13]. These complexes are more effective in lowering the glucose level in blood serum than the inorganic vanadium compounds and are well tolerated in all the animal model of diabetes. Several vanadium complexes with Schiff bases have been reported and their potential in insulin enhancement has been explored [14-17].

Schiff bases are the well-known organic compounds as a result of their manifold biological activities, synthesized by the condensation of aldehydes or ketones and primary amines. This exclusive property is due to the presence of the azomethine linkage and present hetero atom [18, 19]. Recent studies on the antidiabetic activity of Schiff bases and their

complexes have also been tested in animal models, resulting in a significant reduction in blood glucose level and also altered biochemical parameters with improved glucose balance in rats [20, 21].

Coordination chemistry of vanadium

The coordination chemistry of vanadium is dominated with its variable oxidation states which range -I to +V states. A large number of vanadium compounds have been synthesized and characterized using various physicochemical techniques. Most of these vanadium complexes are in higher oxidation states. Many review articles appeared on general coordination chemistry [22-25], structural advances [26], aqueous vanadate chemistry [27] and in other biological systems. Vanadium is important in both reductive and oxidative catalytic transformation in biological systems [28-30].

Vanadium compounds showing insulin-like effects are generally known as insulin mimetics or insulin enhancing compounds. Simple vanadium salts like vanadyl sulphate or sodium metavanadate mimic antidiabetic compounds. The advantage of vanadium compounds relative to insulin is that they may be taken orally. Therefore, the aim of research in the work field of vanadium chemistry is to make vanadium compounds that can approach the target cells with high efficiency. It is now believed that low molecular weight vanadium complexes, should be neutral with optimal lipophilicity to be mobile and cross the cell membrane easily. The VO(ethylmaltolato)$_2$ has successfully crossed the clinical phase I and II tests. It is found that the activities of the vanadium complexes were remains in the range of 30~70% of the activity of insulin. The inorganic salts due to very low oral bioavailability have been synthesized.

In the thesis work, various oxidovanadium(IV/V) of Schiff base complexes have been synthesized and well-characterized using elemental analysis, UV-Vis, FTIR, EPR and the electrochemical (cyclic voltammetry and differential pulse voltammetry) techniques. Finally, these complexes were analysed by single crystal and powder X-ray diffraction techniques to get molecular structures of synthesized complexes. Quantum chemical calculations (DFT studies) suggest a similar structure and same mode for all synthesized complexes. Biochemical assay (antidiabetic activity) demonstrate that these vanadium complexes are potent inhibitors of insulin-mimetic agents. Additionally, a series of dioxidovanadium complexes also synthesized and characterized which are formed by in situ generated Schiff bases.

Chapter 2

Metal-organic hybrids based on a [VO_2(L)]-tecton with cations of imidazole derivatives: Synthesis, characterization and *in vitro* antidiabetic activity

Synthesis of Schiff base (H_2L)

Nicotinic acid hydrazide (1.371 g, 10 mmol) and ortho-vanillin (1.521 g, 10 mmol) were mixed to an ethanol (100 mL) and refluxed for 3 hrs at 80°C. After refluxing the orange solution was cooled to room temperature and the resulting precipitate was filtered and washed with cold ethanol and stored in a $CaCl_2$ desiccator (Scheme 1).

M.P.: 180 °C. Yield: 87 %. Anal. Calc. for $C_{14}H_{13}N_3O_3$ (271.27 g mol^{-1}): C, 61.98; H, 4.83; N, 15.49 %; Found: C, 61.96; H, 4.85; N, 15.51 %. FTIR bands (KBr, cm^{-1}): ν(O–H) 3544 m,

ν(N–H) 3368 w, ν(C=N) 1672 m. ^{1}H NMR (DMSO-d_6, 400 MHz) δ: 12.2 (s, 1H, Ar-OH), 10.8 (s, 1H, –NH), 8.7 (s, 1H, –CH=N-), 6.8-9.0 (m, 7H, Ar-H), 3.82 (s, 3H, -OCH_3), ppm. ^{13}C-NMR (DMSO-d_6, 400 MHz) δ: 161 (C=O), 152 (C=N), 114-148 (Ar-C), 56 (-OCH_3) ppm.

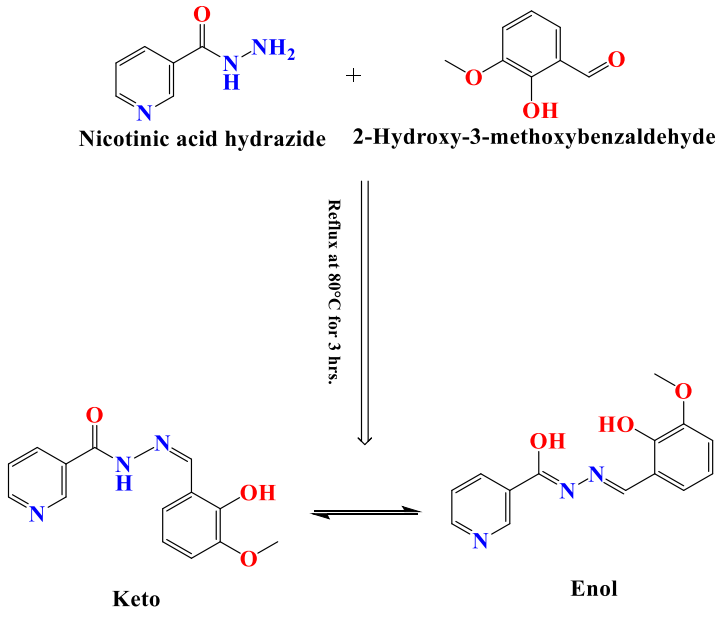

H_2L = (*Z*)-*N*'-(2-hydroxy-3-methoxybenzylidene)nicotinohydrazide

Scheme 1 Structure of Schiff base ligand **H_2L**.

Synthesis of [VO_2(L)]ImH 1

10 mL methanolic solution of vanadium pentaoxide (0.188 g, 1 mmol) was added dropwise to a 10 mL methanolic solution of HL (0.271 g, 1 mmol) at ambient temperature. To this reaction mixture (0.068 g, 1 mmol) ImH (imidazole) was added. The reaction mixture was refluxed for 3 hrs at 80°C, cooled to room temperature. The reaction mixture was allowed to evaporate slowly in the air. After one-week brown crystals of **1** separated, which were collected upon filtration and dried in a $CaCl_2$ desiccator.

Yield: 97 %. Anal. Calc. for $C_{17}H_{16}N_5O_5V$ (421.29 g mol^{-1}): C, 48.46; H, 3.82; N, 16.62 %; Found: C, 48.49; H, 3.85; N, 16.58%. FTIR bands (KBr, cm^{-1}): ν(C=N) 1672 (m), ν(C-O) 1223 (vs), ν(V=O) 951 (s), ν(V-O) 465 (m), ν(V-N) 424 (vs) cm^{-1}. ESI Mass (m/z) = 422.09.

Synthesis of [VO_2(L)]2-MeImH 2

Similarly, complex **2** was prepared by using same procedures as complex **1**. The only difference is in the use of co-ligand that is 2-MeImH (2-methylimidazole) was used in place of imidazole.

Yield: 61 %. Anal. Calc. for $C_{18}H_{18}N_5O_5V$ (435.31 g mol^{-1}): C, 49.66; H, 4.16; N, 16.08 %; Found; C, 49.62; H, 4.14; N, 16.09 %. FTIR bands (KBr, cm^{-1}): ν(C=N) 1635 (m), ν(C-O) 1248 (vs), ν(V=O) 967 (s), ν(V-O) 465 (m), ν(V-N) 424 (vs) cm^{-1}. ESI Mass (m/z) = 436.32.

Synthesis of [VO_2(L)]M-ImH 3

Similarly, complex **3** was prepared by using same procedures as complex **2**. The only difference is in the use of co-ligand that is M-ImH (1-methylimidazole) was used in place of 2-MeImH (2-methylimidazole).

Yield: 71 %. Anal. Calc. for $C_{18}H_{18}N_5O_5V$ (435.31 g mol^{-1}) C, 49.66; H, 4.40; N, 16.05 %; Found: C, 49.62; H, 4.38; N, 16.08 %. FTIR bands (KBr, cm^{-1}): ν(C=N) 1623 (m), ν(C-O) 1254 (vs), ν(V=O) 965 (s), ν(V-O) 474 (m), ν(V-N) 436 (vs) cm^{-1}. ESI Mass (m/z) = 436.08.

Synthesis of $[VO_2(L)]$2-EthImH 4

Similarly, complex **4** was prepared by using same procedures as complex **3**. The only difference is in the use of co-ligand that is 2-EthImH (2-ethylimidazole) was used in place of M-ImH (1-methylimidazole).

Yield: 87 % Anal. Calc. for $C_{19}H_{20}N_5O_5V$ (449.34 g mol^{-1}) C, 50.79; H, 4.49; N, 15.59 %; Found: C, 50.75; H, 4.47; N, 15.56 %. FTIR bands (KBr, cm^{-1}): ν(C=N) 1632 (m), ν(C-O) 1250 (vs), ν(V=O) 942 (s), ν(V-O) 459 (m), ν(V-N) 410 (vs) cm^{-1}. ESI Mass (m/z) = 450.50.

Synthesis of $[VO_2(L)]$BenzImH 5

Similarly, complex **5** was prepared by using same procedures as complex **4**. The only difference is in the use of co-ligand that is BenzImH (benzimidazole) was used in place of 2-EthImH (2-ethylimidazole).

Yield: 95 %. Anal. Calc. for $C_{21}H_{18}N_5O_5V$ (471.08 g mol^{-1}) C, 53.51; H, 3.85; N, 14.86 %; Found: C, 53.48; H, 3.87; N, 14.82 %. FTIR bands (KBr, cm^{-1}): ν(C=N) 1633 (m), ν(C-O) 1281 (vs), ν(V=O) 950 (s), ν(V-O) 459 (m), ν(V-N) 425 (vs) cm^{-1}. ESI Mass (m/z) = 472.11.

Synthesis of $[VO_2(L)]$2-MeBenzImH 6

Similarly, complex **6** was prepared by using same procedures as complex **5**. The only difference is in the use of co-ligand that is 2-MeBenzImH (2-methyl benzimidazole) was used in place of BenzImH (benzimidazole).

Yield: 90 %. Anal. Calc. for $C_{22}H_{20}N_5O_5V$ (485.37 g mol^{-1}) C, 54.44; H, 4.15; N, 14.43 %; Found: C, 54.41; H, 4.17; N, 14.40 %. FTIR bands (KBr, cm^{-1}): ν(C=N) 1633 (m), ν(C-O) 1280 (vs), ν(V=O) 947 (s), ν(V-O) 470 (m), ν(V-N) 442 (vs) cm^{-1}. ESI Mass (m/z) = 486.19.

Results and discussion

The Schiff base was obtained by mono condensing of equimolar ethanolic solution of nicotinic acid hydrazide and o-vanillin (Scheme 1). Six new complexes of dioxide ((Z)-N'-(2-hydroxy-3-methoxybenzylidene) nicotine hydrazide) vanadate(V) salts with Imidazole (ImH), 2-methylimidazole (2-MeImH),1-methylimidazole (M-ImH), 2-ethylimidazole (2-EthImH), benzimidazole (BenzImH) and 2-methylbezimidazole (2-MeBenzImH) counter ions were synthesized using Scheme 2 and 3 in good yield. Yellow coloured polycrystalline complexes were obtained. These were characterized using elemental analysis, FTIR, single X-ray analysis and NMR techniques. All the complexes are air-stable. The complexes are insoluble in water, hexane, benzene and petroleum ether but soluble in DMSO, DMF, and acetonitrile. The room temperature magnetic susceptibilities values indicate the diamagnetic character of these complexes. Thus, all complexes are in a +5-oxidation state. Several efforts for recrystallization for complexes **3**-**6** were made but, single crystals suitable for X-ray analysis were not obtained. These complexes were also tested for antidiabetic activity. We have also done computational study also.

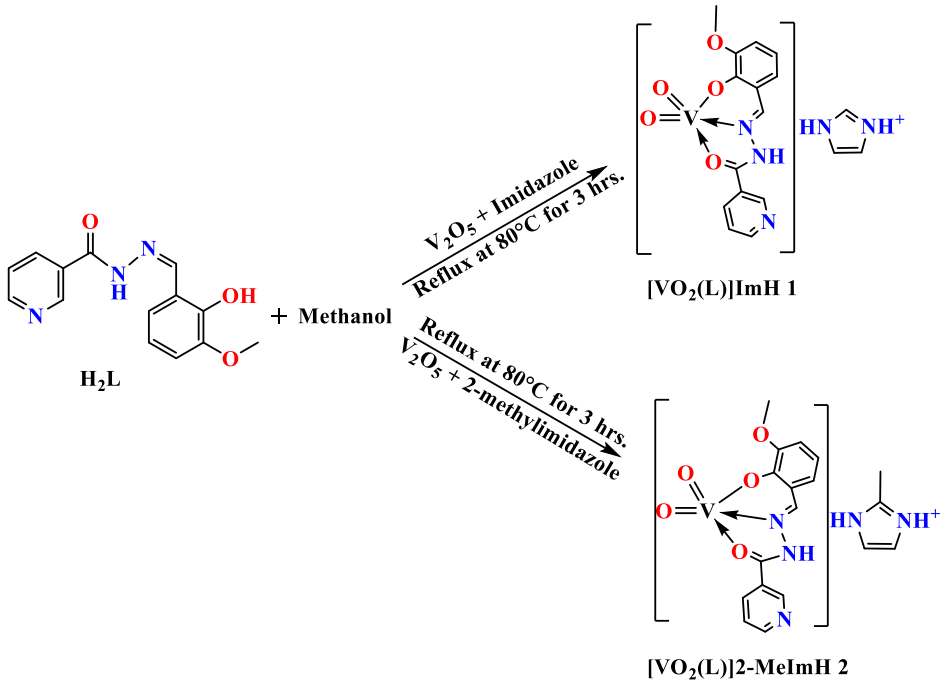

Scheme 2 Synthetic route of complexes **1** and **2**.

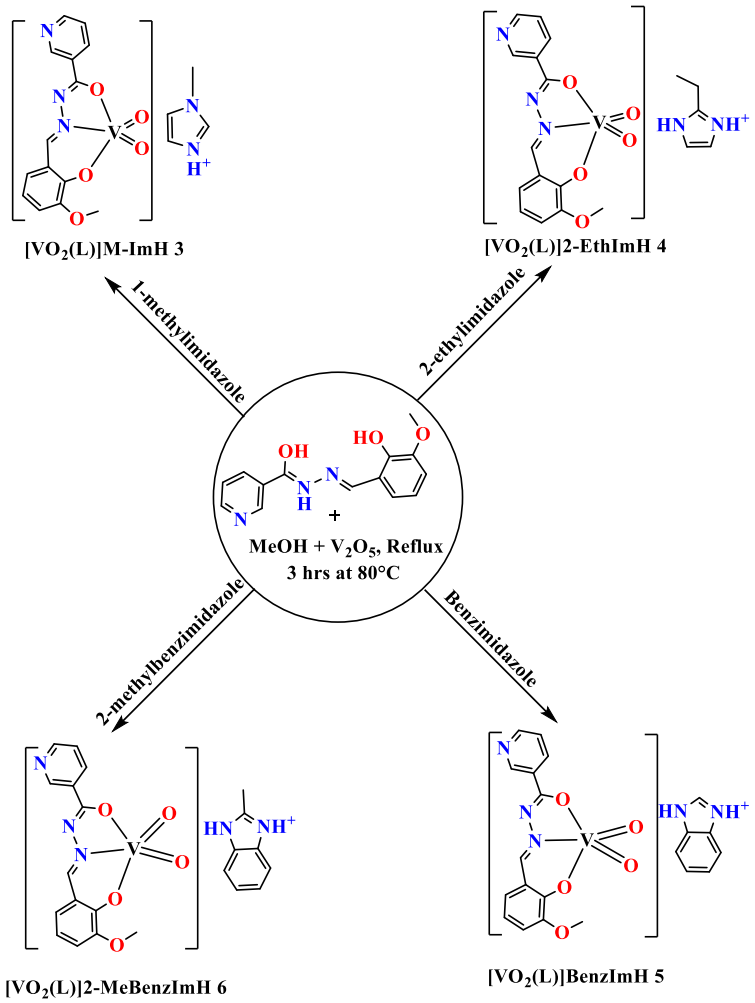

Scheme 3 Synthetic route of complexes **3-6**.

NMR spectral study

The ^{1}H NMR spectra of Schiff base (H_2L) have been recorded in DMSO-d_6. The phenolic (-OH) protons of the H_2L appeared at 12.2 ppm and hydrazide (-NH-) proton appear in 10.8 ppm. The spectrum shows a peak at 8.7 ppm which is assigned to azomethine (-CH=N-) proton. Thus, the ligand spectrum of the Schiff base suggests existing only enol form in solution. ^{13}C NMR Carbonyl (-C=O) and azomethine (-CH=N-) carbon peak is indicated in 161 and 152 ppm. The (-CH-OCH_3) peak was obtained at 124 ppm. Similarly, aromatic peaks are obtained in the range of 114-148 ppm. ^{13}C NMR of ligand H_2L methyl (-OCH_3) carbon peak appeared in 56 ppm.

Magnetic susceptibility

The room temperature susceptibilities values reveal the diamagnetic nature of complexes **1-6**, conforming to the +5-oxidation state of the vanadium centre (d^0).

Molar conductance

The molar electrical phenomena values of complexes **1-6** were also measured in 1.0×10^{-3} M DMSO solution. The observed range of molar conductance is 70.86-84.21 Ω^{-1} cm^2 mol^{-1}. These values are lower than the molar conductance for a 1:1 electrolyte.

FTIR Spectra studies

The FTIR spectra of complexes were recorded in the 400-4000 cm^{-1} range in the KBr pellet. A comparison of the FTIR spectral data with these of the complexes reveals that the H_2L ligand is coordinated to the vanadium ions in the enol form in complexes. The FTIR spectrum of the H_2L ligand show stretching vibration at 3270 due to ν(N-H) stretching respectively. The disappearance of this band in complexes suggests the replacement of proton (H) by the vanadium ion. The bands appearing in the range 1250-1280 cm^{-1} are assigned to the ν(C-O $_{enolic}$) mode. The stretching vibration of the >C=N group, which shifts to lower wave number in complexes, suggestive of the coordination of the azo-methine nitrogen to the vanadium centre. The strong new bands found in complexes in the region at 947-950 cm^{-1} are assigned to V=O group stretching vibrations, indicating the dioxidovanadium of the vanadyl group. Two weak nonligand bands as shown in appear in the low wave number region 453-473 cm^{-1} and 410-442 cm^{-1} due to ν(V-O) and ν(V-N) stretching vibrations respectively.

Electronic spectral studies

Electronic spectra of both complexes were recorded using DMSO solutions [3×10^{-3} M] at RT. Spectral features of both complexes **1** and **2** are almost similar. The electronic spectra of complexes are possibly due to the ligand-to-metal charge transfer (LMCT) to empty d-orbitals of the metal. As vanadium(V) complexes possess a d^0 configuration, d-dbands are not expected for the present complexes.

Electrochemistry studies

Electrochemical studies of these complexes were also explored using cyclic voltammetry (CV). The cyclic voltammetry of complexes **1** and **2** have been recorded in DMSO solution (1.0×10^{-3} M) using 0.1 M tetrabutylammonium perchlorate (TBAP) as a supporting electrolyte with Ag/AgCl as the reference electrode. CV experiments of **1** exhibited V^{V}/V^{IV} reductive responses with potential fairly on the negative side (-0.754 V). Its anodic counterpart is not visible. In complex **2** no such reduction wave was observed. We believe that the presence

of an electron-donating methyl group in substituted imidazole in this complex increased the electron density at the vanadium centre and therefore better stabilize the V^V state.

Mass spectral analysis

The ESI-Mass of complexes **1-6** were carried out to get information about the molecular weight of the complexes. The mass of these complexes was matched with calculated values. The mass of complexes gives the molecular ions peaks in the form of $[M]^+$ and $[M + 1]^+$ ion in the positive mode ESI-Mass.

X-ray structures of complexes 1 and 2

Crystal structure of Complex 1

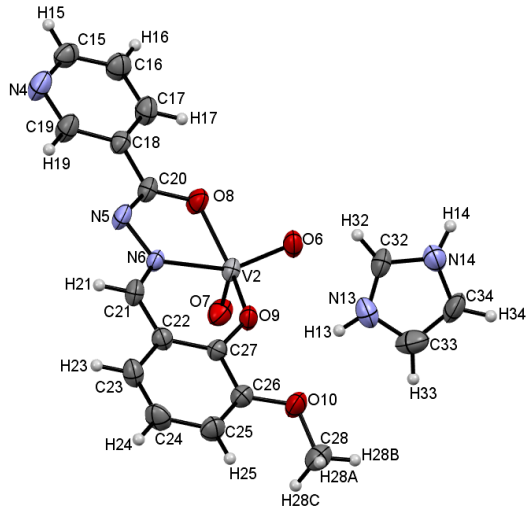

Complex **1** crystallizes in the *P-1* triclinic space group.In the structure of this complex, the vanadium metal is pentacoordinate by two oxido groups and monoanionic tridentate ONO Schiff base ligand. The coordination sphere of vanadium is distorted pyramidal, as ascertained by the structural parameter $\tau_5 = 0.024$ (0 for an ideal square pyramid and 1 for an ideal trigonal bipyramid). One imidazole molecule as lattice remains out the V^V coordination sphere. In the lattice of the complex, strong bifurcated intermolecular H-bonding interactions (N···O distances: 2.226-2.246 Å) between the Schiff base oxygen atoms (O5, O6, O9 and O10) and the -NH- groups of imidazole.

Crystal structure of Complex 2

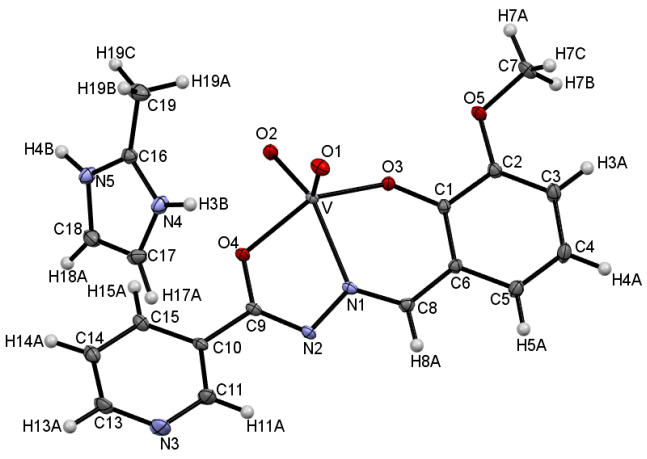

The crystal structure of this complex consists of a vanadium atom pentacoordinate by monoanionic tridentate Schiff base (L^-) and two dioxide group. In the crystal structure of this complex 2-methylimidazole remains as a lattice molecule. Again, in this complex coordination geometry is a distorted square pyramidal, as ascertained by the structural parameter $\tau_5 = 0.04$.In this complex, each 2-methyimidazole moiety forms H-bonds of various types. N-H hydrogen atoms of 2-methyimidazole yield bifurcated robust intermolecular H-bonding with O of oxido L^-.

Thermal analysis

Thermal decomposition studies of complexes **1** and **2** were carried out in the nitrogen atmosphere at temperatures ranging from 25 to 600 °C to determine their decomposition patterns. Metalloid complexes have been found to be more stable than ligands. The TG graphs of the $[V(O)_2(L)]$ImH **1** and $[V(O)_2(L)]$m-ImH **2** complexes. The decomposition of complexes can be seen in three stages on the thermogram. The decomposition pattern is shown in Scheme 4. In the first step, complexes **1** and **2** lose 3.0% and 10 % at 100-250 °C of its weight with separation of methoxy group present in the ligand moiety.

Antioxidant activity

The result of the *in vitro* antioxidant activity of **H_2L**, **1** and **2** is presented. The IC_{50} was calculated for DPPH radical scavenging assay. The IC_{50} values of **H_2L** and complexes **1** and **2** were 729.26, 422.58 and 441.40 µg/ml respectively, whereas that of ascorbic acid was 730.12 µg/mL. The DPPH scavenging activity was lower than that of positive control ascorbic acid, while higher than that of **HL**. Wazalwar and co-workers reported a similar DPPH scavenging activity of vanadium(V) complexes. These results showed that the complexes have the potential in scavenging free radicals. Reactive oxygen species (like, O_2^-, H_2O_2 etc.) were major by-products of oxidative metabolism in the mammalian system.

α-Glucosidase inhibition activity

The Schiff base H_2L and complexes **1** and **2** showed inhibitory activity against α-glucosidase. Following the *in vitro* experiments, the IC_{50} values of H_2L, **1** and **2** were 26.89, 153.03 and 32.54 µg/mL respectively. H_2L and **2** showed low IC_{50} values towards the inhibition of α-glucosidase and these values are similar to that of the control acarbose. These results showed that the H_2L, **1** and **2** complexes were a potent inhibitor against α-glucosidase. These observations are consistent with the results of reported similar vanadium complexes. The complexes **3-6** were IC_{50} values of each determined from the inhibition plot between % inhibition *vs.* concentrations. The concentration-dependent activity of α-glucosidase was observed in all complexes. Although the IC_{50} of present complexes is less than the control acarbose (standard). The observed trend in is: **4** > **3** > **6** > **5**. The geometry of present complexes is distorted square planar, these may be α-glucosidase at the active site.

α-Amylase Inhibition

α-Amylase plays a major role in the hydrolysis of starch to maltose. Hence, the inhibition of α-amylase is a strategy for the management of diseases such as diabetes and obesity. Found lowest IC_{50} value is 23.67 in **1** (23.669 ± 15.07) while the highest IC_{50} in **2** (182.901 ± 285.3) and moderate in H_2L IC_{50} (56.7959 ± 14.58). It was thus revealed that complex **1** showed the highest *in vitro* α-amylase (insulin-mimetic) activity among compounds examined in this study. These complexes showed the trends of IC_{50} similar to the trend observed for α-amylase activity measurements. Complex **3** revealed the highest amylase

activity. This complex is the softest and the smallest ΔE being most active. The present complexes have shown better inhibition activity against the α-amylase enzyme. The distorted square pyramidal geometry of the complexes may bind the active site through hydrogen bonding or other hydrophobic interactions.

β-Glucosidase activity

This is an important finding because sweet almonds have β-glucosidase. Hence, these compounds have a positive effect on the sweet almonds β-glucosidase similar to the reported findings of vanadyl complexes. The β-glucosidase inhibitory activity of H_2L, **1** and **2** were investing ahead of and presented. The IC_{50} value of β- glucosidase inhibition was found lowest in sample H_2L (19.5252 ± 13.44) while highest in 2 (2021.77 ± 5.547) and moderate in complex **1** (282.05 ± 1.284).

Hirshfeld Surface Analysis (HSA)

Molecular Hirshfeld surfaces in the crystal structure were constructed based on the electron distribution calculated as the sum of spherical atom electron densities. For a given crystal structure and a set of spherical atomic densities, the Hirshfeld surface is unique. The normalized contact distance (d_{norm}) based on both d_e and d_i (where d_e is the distance from a point on the surface to the nearest nucleus outside the surface and d_i is the distance from a point on the surface to the nearest nucleus inside the surface) and the vdW radii of the atom, as given by eq 1 enables identification of the regions of particular importance to intermolecular interactions. The combination of d_e and d_i in the form of a two-dimensional (2D) fingerprint plots. Provide a summary of intermolecular contacts in the crystal.

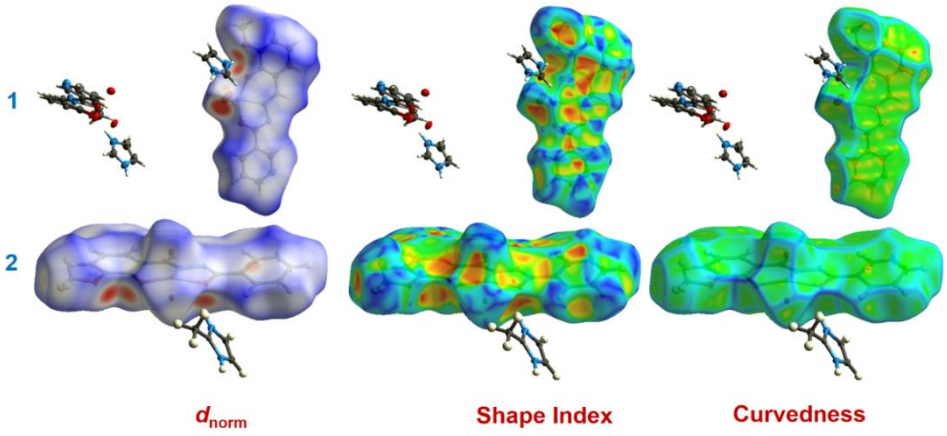

Hirshfeld surfaces mapped with d_{norm}, shape index and curvedness for the complexes **1** and **2**.

Computational studies of complexes

The electronic structure of complexes correlating the experimental bond distances and angles was investigated by the DFT calculations using B3LYP functional. The experimental single-crystal X-ray analysis data bond distances and angles are in good agreement with calculated data. However, some bond distances and angles deviate significantly from those obtained from the single-crystal X-ray diffraction data. The difference in data is an expected result because geometrical optimizations are performed in the gaseous state in which intermolecular interactions are absent.

Mulliken spin population analysis

Mulliken spin population analysis is also performed to determine the partial atomic charges. These charges yield important information about the origin of molecular properties including dipole moments and molecular polarizability. Although, it has been used to describe the electrostatic potential surfaces in molecular structure. In the spin density plot green lobes show positive spin density whereas blue lobes show negative spin density.

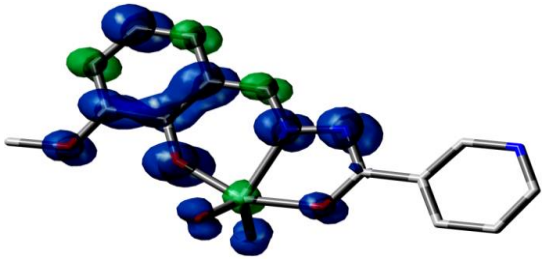

HOMO-LUMO Analysis

The HOMO-LUMO analysis of complexes **3-6** were carried out. The frontier molecular orbitals (FMO) highest occupied molecular orbital (HOMO) and lowest unoccupied molecular orbital (LUMO), can be applied to discuss electron donors and acceptors, which control the bioactivity and decide the way a molecule interacts with the biological systems. The investigation on their frontier molecular orbitals can reveal useful information for the working mechanism of the bioactive compounds, such as active sites.

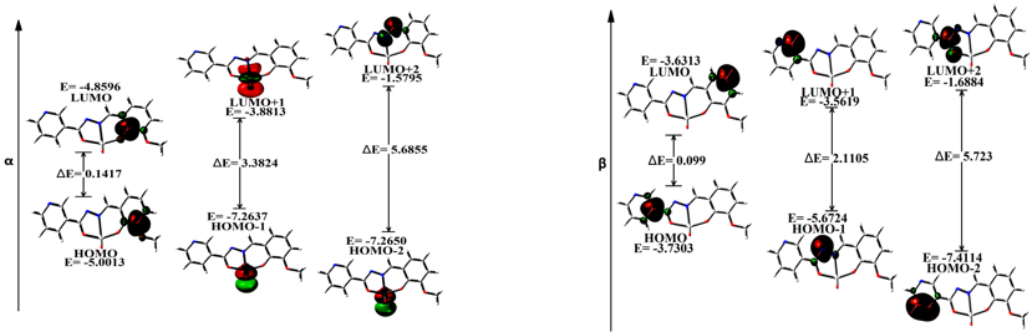

HOMO-LUMO energies and energy gap of complex **1**.

Quantitative structure-activity relationship (QSAR)

Associated quantum chemical (crucial electronic) parameters of present complexes were also calculated. The objective of the present structure-activity relationship study is to correlate the biological activities of complexes with the most effective quantum chemical molecular descriptors. The analysis of results of crucial electronic parameters shows that the hardness decreases and softness increase following this trend: **5**, **6**, **3** and **4** which reveals that the charge transfer process is more predominant in **5** compared to other complexes.

Conclusions

Schiff base ligand H_2L N'-(2-hydroxy-3-methoxybenzylidene) nicotinohydrazide have been prepared and characterized by FTIR, ^{1}H and ^{13}C NMR. In this work, six oxidovanadium(V) complexes of tridentate Schiff base ligand H_2L N'-(2-hydroxy-3-

methoxybenzylidene) nicotinohydrazide having donor site ONO was synthesized and characterized by a various physicochemical and spectroscopic techniques such as elemental analysis, FTIR, UV-Vis, CV, DPV and DFT calculations. In all complexes, the V(V) center is coordinated vanadium metal is pentacoordinate by two oxido groups and monoanionic tridentate ONO Schiff base ligand. The structure of the H_2L ligand and complex **1** and **2** were determined by single crystal X-ray diffraction. Room temperature magnetic susceptibility measurement indicated that the complexes are diamagnetic. In the UV-Visible spectrophotometry d-d bands are not shown in present complexes, due to $3d^0$ configuration. In-vitro α-glucosidase inhibition activity and α-amylase inhibition activity results proved that these complexes are promising anti-diabetic agents.

Chapter 3

New oxidovanadium(IV/V) complexes with tridentate Schiff base ligands: Synthesis, molecular structure and *in vitro* antidiabetic activity

Synthesis of ligand HL^1

To a solution of acetyl hydrazide (0.7g, 10 mmol) in ethanol (20 mL) was added with stirring to a solution of vanillin (1.521 g, 10 mmol) in ethanol (50 mL) and heated under reflux for 2 hrs at 80 ºC (Scheme 1). The solvent was removed under reduced pressure and a light-yellow solid resulted. Finally obtained Schiff base was washed with ethanol and recrystallized from ethanol.

M.P.: 175 ºC. Yield: 87 %. Anal. Calc. for $C_{10}H_{12}N_2O_3$ (208.23 g mol^{-1}): Calc. C, 57.68; H, 5.81; N, 13.45 %. Found: C, 57.71; H, 5.83; N, 13.42 %. FTIR bands (KBr, cm^{-1}): ν(C=N) 1679 m, ν(-OH) 3433 b, ν(N-H) 3015 m. ^{1}H NMR ($CDCl_3$, 400 MHz) δ: 10.4 (s, 1H, Ar-OH), 10.2 (s, 1H, –NH), 8.01 (s, 1H, –CH=N), 6.8-7.2 (m, 3H, Ar-H), 3.9 (s, 3H, -OCH_3), 2.3 (s, 3H -$COCH_3$) ppm. ^{13}C NMR (DMSO-d_6, 400 MHz) δ: 165 (C=O), 147 (CH=N), 113-148 (Ar-C), 56 (-OCH_3), 21.8 (-$COCH_3$) ppm.

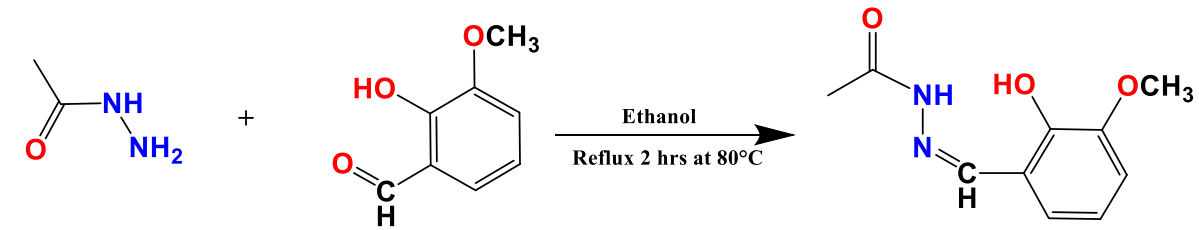

Acetyl Hydrazide **O-vanillin** **HL^1**

Scheme 1 Synthetic route of ligand **HL^1** = (Z)-N'-(2-hydroxy-3-methoxybenzylidene)acetohydrazide.

Similarly, **HL^2- HL^4** ligands were synthesized using same procedure as ligand **HL^1**.

Synthesis of ligand HL^2

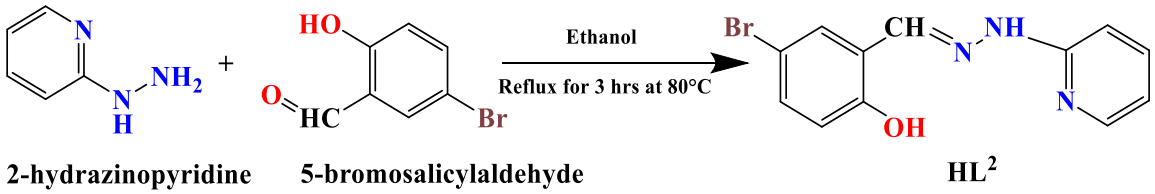

Scheme 2 Synthetic route of **HL^2** = (E)-4-bromo-2-((2-(pyridin-2-yl)hydrazono)methyl)phenol.

Synthesis of ligand HL^3

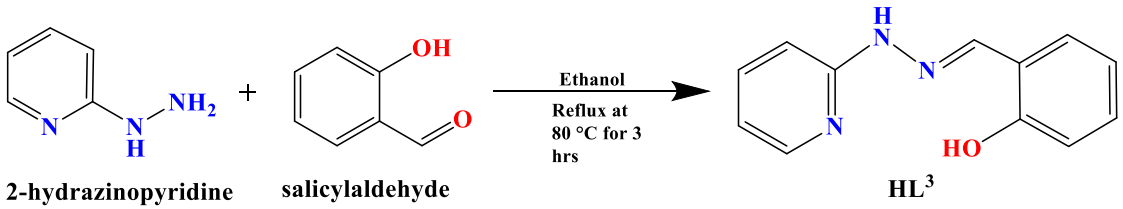

Scheme 3 Synthetic route of **HL^3** = (E)-2-((2-(pyridin-2-yl)hydrazono)methyl)phenol.

Synthesis of ligand HL^4

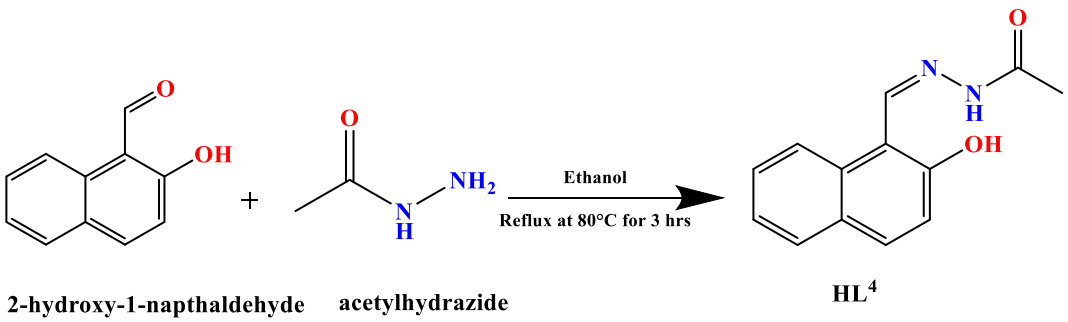

Scheme 4 Synthetic route of **HL^4** = (Z)-N'-((2-hydroxynaphthalen-1-yl)methylene)acetohydrazide.

Synthesis of $[VO(L^1)(H_2O)]NO_3$ 1

Vanadyl sulphate monohydrate (0.163 g, 1 mmol) in 10 ml water and Schiff base HL^1 (0.208 g, 1 mmol) in 10 mL methanol were mixed and stirred for 1hrs at ambient temperature. Then 1 mmol sodium nitrate in 5 mL water was added and reflux for 3 hrs 80 ºC. After 2 to 3 hrs burgundy colour solid was separated and filtered off, washed with methanol. Finally, complex dried in a $CaCl_2$ desiccator.

Yield: 87 %. Anal. Calc. for $C_{10}H_{13}N_3O_8V$ (354.17 g mol^{-1}): Calc. C, 33.91; H, 3.70; N, 11.86 %. Found: C, 33.92; H, 3.72; N, 11.84 %. FTIR (KBr, cm^{-1}): ν(C=N) 1633 vs, ν(V=O) 964 vs, ν(V-O) 581 m, ν(V-N) 540 vs.

Similarly, all other complexes (**2-7**) were synthesised. The synthetic route of all complexes is given scheme 5 and 6.

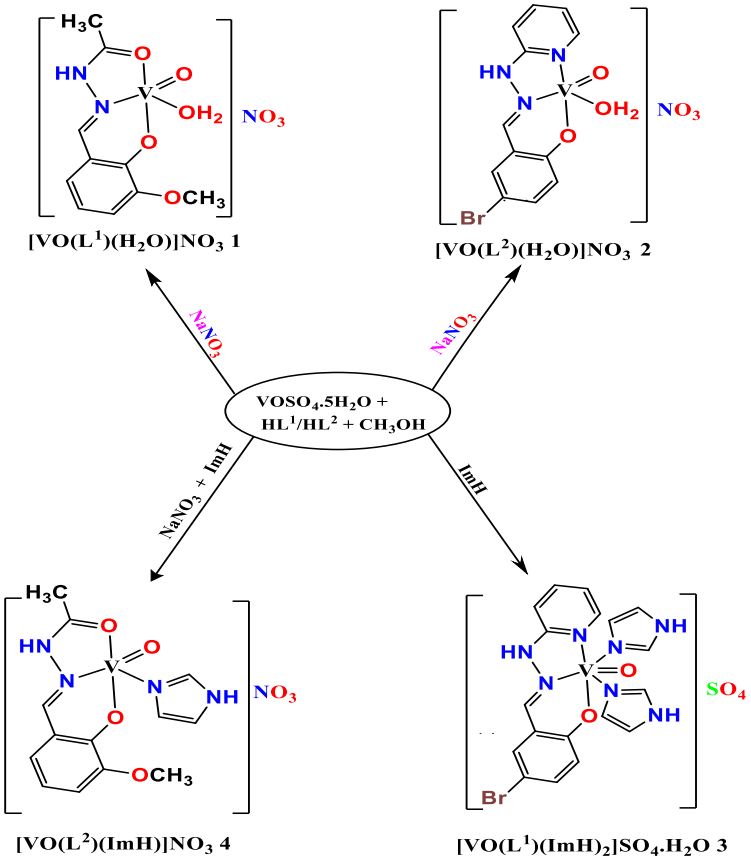

Scheme 5 Synthetic route of complexes **1-4**.

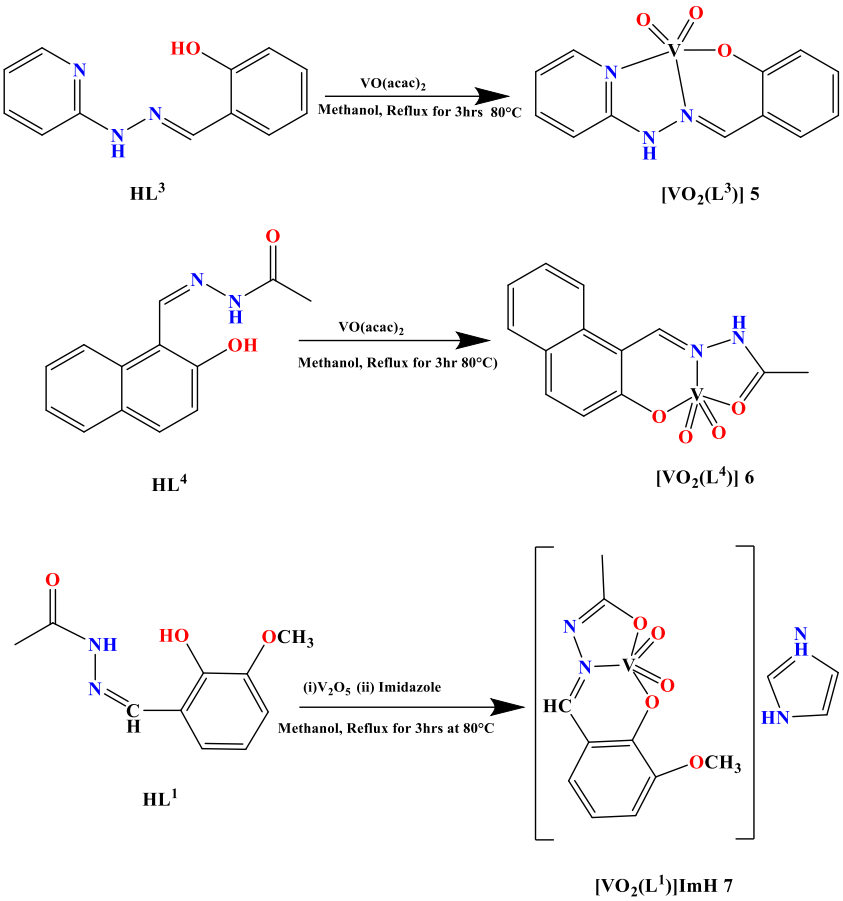

Scheme 6 Synthetic route of complexes **5-7**.

NMR spectra of Ligands

The proton NMR of ligands HL^1, HL^2, HL^3 and HL^4 were recorded in $CDCL_3$ solvent at room temperature. Proton NMR spectra of the ligands showed a sharp signal (singlet) in the range between 8.01-8.81 ppm, which can be assigned to the azomethine proton. Similarly, hydroxyl proton (OH) is obtained in the range of ~ 10.4-10.8 ppm. Hydrazide N-H proton appear in the range of 8.7-10.2 ppm. In ligands, the aromatic proton peaks are observed in the range of 6-8 ppm. In ligand HL^1 and HL^4 methyl ($-COCH_3$) proton appears at 2.364 and 2.426 ppm respectively. The ^{13}C NMR spectra of the ligands were recorded in DMSO-d_6. Similarly, carbonyl (C=O) carbon peaks and azomethine carbon (CH=N-) are obtained in the range of ~ 165 and 146 ppm. Similarly, aromatic carbon peaks are obtained in the range of 106-157 ppm. In ^{13}C NMR of ligand HL^1 and HL^4 methyl, ($-CH_3$) carbon peaks appear at ~ 21.82 ppm.

FTIR Analysis

All Schiff bases ligand (HL^1-HL^4) show strong bands in the region 3411-3441 cm^{-1} and 3017-3127 cm^{-1} which are assigned to ν(OH) and ν(N-H) respectively. The stretching frequency for azomethine ν(C=N) in the ligand is between the range 1633-1679 cm^{-1}. The absence of ν(OH) band at a 3400 cm^{-1} in the corresponding metal complexes due to deprotonation upon coordination. In complexes, the ν(C=N) bands are now located at 1601-1657 cm^{-1}, indicating complexation of azomethine nitrogen to the vanadium. A new band around ~1596±2 cm^{-1} in all complexes is assigned to the ν(C−O) vibration. In complexes,**1**, **2**, and **4** ν(NO_3) is seen at ~1405, 1378 and 821 cm^{-1} indicating the ionic nature of nitrate anion.

Similarly, in complex **3** a sharp band at 1365 cm^{-1} is due to sulphate ion. All complexes show one sharp band at around ~ 949-988 cm^{-1} assigned to stretching vibration of oxidovanadium moiety ν(V=O).

Electronic spectra

Electronic absorption spectra of complexes **1-7** were recorded in a DMSO solution (3.0 × 10^{-3} M). Electronic spectroscopic data for the complexes in DMSO solution are summarized. Complexes **1**, **2** and **4** show visible band in the range 765-810 cm^{-1} along with UV band. A strong band around 411 nm in complexes **1**, **2**, and **4** correspond to the ligand to metal charge transfer (LMCT) transitions originating from the p_x orbital of phenolate oxygen to the empty d orbital [PhO→V_{dx}] of the vanadium(IV) center.

Molecular structure of ligand HL^2

The molecular structure of HL^2, Crystal data and structure refinements are listed. The HL^2 has three donors (NNO) sites, *viz.*, phenolic oxygen (O1), imine nitrogen (N2) and pyridine nitrogen (N3). The phenol C1-O1(-H) bond of 1.32(2) Å is within the limit of a C-O single bond. The bromine and pyridine atoms in the Schiff base are involved in the intramolecular hydrogen bondings.

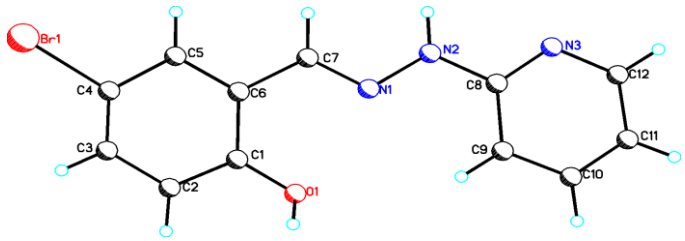

Molecular structure of complex 3

In the molecular structure, the vanadium ion has an N_4O_2-donor environment, arranged in a distorted octahedral geometry. One of the imidazole rings is disordered over two sets of sites in a 0.55(1):0.45(1) ratio. It's not disordered over a two-fold rotation axis but is disordered over two positions because the S atom is positioned at the inversion center. Half solvent molecule (half water molecule) was also observed. The solvent molecule lies on a two-fold axis. In structure refinement, an oxygen atom of water solvent has only 50% occupancy. Atom O711 of water solvent is further disordered to another position O712 with refinable occupancy, constrained to add up to 0.5. Water hydrogen could not be located due to disorder. The equatorial plane consists of N1, N6, N211 and O2 atoms. While the oxido oxygen atom O1 and the nitrogen atom of azomethine N13 of L^- occupies the axial positions.

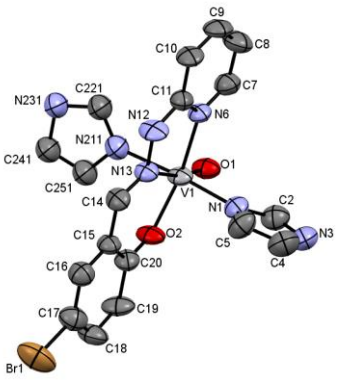

Molecular structures of complexes 5-7

The molecular structures of complexes **5**, **6** and **7** have been solved using single-crystal X-ray analysis. The X-ray analysis displayed that complex **5** is crystallized in the Pc2a1 space group as a racemate. The molecular geometry of **5** in crystals with the atom labelling. Additional crystal data along with more information about the X-ray structure analyses. This complex consists of a dimer with two independents asymmetric (molecules) units. The monoanionic tridentate ligand (HL^3) spans the meridional sites through pyridine and imino nitrogen's and phenolate oxygen the basal plane and two dioxido groups at the apical position forming a five coordinated geometry.

Hirshfeld surfaces analysis of complexes 3

The Hirshfeld surfaces analysis of complexes **3**, **5**, **6** and **7** were done for guessing the interactions in the formation of supramolecular architecture. To gain an idea about the molecular framework especially the aromatic and chelate rings the surfaces are plotted as transparent. The d_{norm} surface is mapped between -0.25 to 1.25 Å range, shape index plots are constructed between -0.8 to 0.8 Å while curvedness plots are mapped in the range -3.0 to 0.3 Å. In this complex, the O···H interactions as described in crystal structure description (vide supra) can be seen as the large circular deep red depressions and the weaker π···π interactions are shown as the faint red shaded area. Another salient result of the Hirshfeld surface analysis is the fingerprint plots which are useful for analysing the relative contribution of different intermolecular contacts.

Magnetic and EPR spectral study

Room temperature magnetic measurements of complexes **1**, **2** and **4** were performed. The complexes **1**, **2** and **4** show magnetic moment of 1.79, 1.77 and 1.83 BM respectively in accord with a spin only value of a d^1 the system, whereas vanadium(V) complex **3**,**5**, **6** and **7** which are d^0 system is diamagnetic. The magnetic moment values of **1**, **2** and **4** are in agreement with EPR results. The complexes **1-4** were also characterized by EPR spectral measurements at room temperature (RT) and liquid nitrogen temperature (LNT) by dissolving complexes in DMSO. The EPR parameters from isotropic and anisotropic spectra for oxidovanadium (IV) complexes were evaluated from the experimental EPR spectrum.

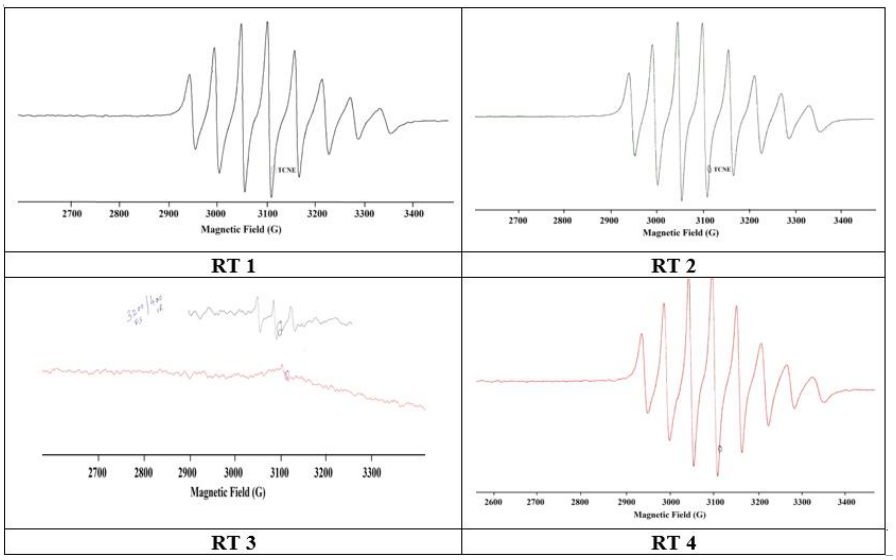

EPR spectra of complexes **1-4** at Room temperature.

Cyclic Voltammetry

The electrochemical behaviour of all complexes was studied in DMSO solution (3.0×10^{-3} M) using cyclic voltammetry (CV). Tetra butyl ammonium perchlorate (TBAP) was used as a supporting electrolyte. The results of the cyclic voltammetric studies for oxidovanadium(IV/V) complexes are presented in Table 13. The cyclic voltammetric studies in DMSO reveal a one-electron reduction process in the range of -0.73 to -0.84 V.

Theoretical calculations

To gain insight into the electronic structures of complexes full geometrical optimization of complexes **1-4** was performed. The optimized geometrical parameters (bond lengths and angles), Mullikan densities and charges, global reactivity parameters and energies of frontier molecular orbitals (FMO) were computed and analyzed. From the elemental analysis (C, H, N) and spectroscopic experimental data, it is proved that vanadium ions coordinated to the tridentate Schiff base *via* N and O atoms forming the complexes **1** and **2** whereas in **3** and **4** co-ligand imidazoles are also coordinated. Molecular structures of **3** are also analyzed by single-crystal X-ray analysis.

HOMO-LUMO analysis

The frontier molecular orbitals (FMO), highest occupied molecular orbital (HOMO), lowest unoccupied molecular orbitals (LUMO) are used to ascertain electron donors and acceptors. These parameters affect the bioactivity and give an idea about the way a molecule interact with the biological species. The research on their FMO can yield knowledge for the operating mechanism of the biologically active compounds.

Mulliken charge analysis

The Mulliken charge analysis of present complexes was also performed and listed in Table 16. It is established that the atomic charge populations of a molecule are well correlated to active sites in its electrophilic or nucleophilic reactions and the charge interactions between two species, such interactions can show the functional role in inhibiting the growth of fungi. On perusal of Mulliken population data, it is apparent that the coordination leads to the redistribution of electron density in the coordinated moieties.

Global chemical reactivity indices of complexes 1-4

Density functional theory yields the important molecular descriptors. These descriptors decide the structural stability and reactivity of a molecule. From the energies of frontier molecular orbitals (FMO), the highest occupied molecular orbitals (HOMO) and lowest unoccupied molecular orbitals (LUMO) are useful in deciding some global reactivity parameters of molecules. These are electronic chemical potential (μ), electro-negativity (χ), ionization potential (I) and electron affinity (EA). The electronic chemical potential (μ) of a molecule is the escaping tendency of electrons from a molecule, the negative value of μ reveals that the molecule does not decompose spontaneously into its constitutional elements. Global hardness decides the resistivity of molecules.

Molecular Docking

For complex **1** of protein receptor with vanadium derivative, the binding energy observed was -4.940 Kcal/mol and ligand was observed to form five favourable interactions with alpha glucosidase. For complex **2** of protein receptor with vanadium derivative-2, the

binding energy observed was -4.612Kcal/mol and ligand was observed to form six favourable interactions with the receptor. For complex **3** of protein receptor with vanadium derivative-3 the binding energy observed was -4.91Kcal/mol and ligand was observed to form seven favourable interactions with the receptor. For complex **4** of protein receptor with vanadium derivative-4, the binding energy observed was -4.41Kcal/mol and ligand was observed to form four favourable interactions with the receptor.

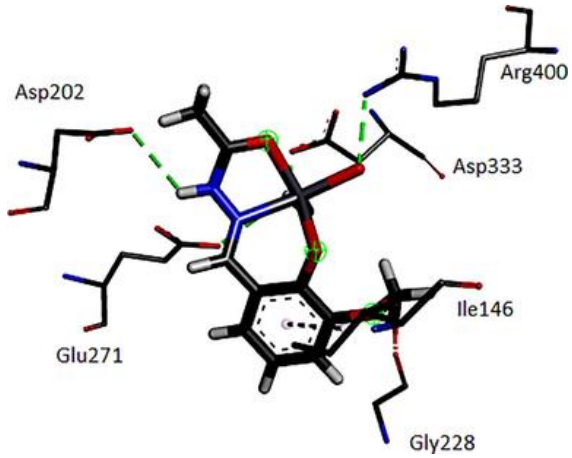

Complex 1

α-Glucosidase inhibition activity

The activity of HL^1, HL^2, complexes **1-4** were carried out, against alpha glucosidase and inhibition graph. We found lowest IC_{50} value for **1** while highest IC_{50} were found in HL^2 and moderately in **2, 3** and **4**. The IC_{50} values for α-glucosidase inhibition activity were ranged from 4-400 µg/mL **2** observed most potent among all the complexes with IC_{50} value 4 µg/mL while HL^2 was cheapest inhibitor with IC_{50} value 432 µg/mL. The α-glucosidase activity of HL^3, HL^4, **5**, **6** and **7** were also measured against α-glucosidase. The percentage inhibition plots of these compounds, IC_{50} and α-glucosidase activity are collected. It is observed that the IC_{50} values of complexes are lower in comparison to the corresponding free ligands.

α-Amylase Inhibition

In the present study activity of HL^1, HL^2, complexes **1-3** were carried out against alpha amylase and the inhibition graph is shown. Lowest IC_{50} value observed in **1** while the highest IC_{50} were found in HL^2, **2** and **3** showing moderate inhibition against α-amylase at different concentration. The α-amylase inhibitory data of ligands activity HL^3 and HL^4 and their complexes (**5-7**) with vanadium were performed by the reported. In the same table α-amylase inhibitory is also indicated for each ligand and complexes. It can be seen from that complexes showed better inhibitory activity in comparison used ligands. α-amylase performs a major role in the useful in reducing postprandial hyperglycaemia and then controlling diabetes or obesity.

Conclusions

In this work, we have synthesized HL^1, HL^2, HL^3 and HL^4 hydrazide ligand and characterized by FTIR, ^1H and ^{13}C NMR. a series of vanadium (IV/V) complexes **1**-7 of tridentate Schiff bases were synthesized and characterized by various physicochemical methods such as elemental analysis, FTIR, UV-Vis, CV and EPR techniques. The structures determined on ligand HL^2, complex **3, 5, 6** and **7** by single-crystal X-ray diffraction. The geometry of five coordinated complexes (**1**, **2**, **4**, **5**, **6** and **7**) can be described in terms of

trigonal bipyramidal or square pyramidal. The room temperature magnetic measurements of complex **1**, **2** and **4** are in the range of 1.79 to 1.83 B.M. The molecular structure of complex **3** shows that the central metal ion has an N_4O_2-donor environment and has octahedral geometry. *In-vitro* α-glucosidase inhibition activity and α-amylase inhibition activity results proved that these complexes are promising anti-diabetic agents.

Chapter 4

Anionic dioxidovanadium(V) complexes $[VO_2(L)]^-$ with (Z)-N'-(2-hydroxy-3-methoxybenzylidene) isonicotinic hydrazide as proligand and cation of imidazole units as ancillary ligands: Synthesis, characterization and *in-vitro* antidiabetic activity

Synthesis of Schiff base (H_2L)

To the ethanolic solution (30 mL) of isonicotinic acid hydrazide (1.371 g, 10 mmol) an ethanolic solution (30 mL) of o-vanillin (1.521 g, 10 mmol) was added with 2-3 drops of glacial acetic acid as a catalyst and refluxed for 1 hrs. After refluxing 1 hrs the orange solution was cooled to room temperature and the resulting precipitate was filtered and washed with cold ethanol and dried in a $CaCl_2$ desiccator (scheme 1).

Yield: 87 %. Anal. Calc. for $C_{14}H_{13}N_3O_3$ (271.27 g mol^{-1}) C, 61.98; H, 4.83; N, 15.49 %. Found: C, 61.95; H, 4.85; N, 15.50 %. FTIR bands (KBr, cm^{-1}): ν(O–H) 3440 s, ν(N–H) 998 (vs), ν(C=N) 1691(vs). ^{1}H NMR (DMSO-d_6 400 MHz) δ: 12.2 (s, 1H, Ar-OH), 10.8 (s, 1H, –NH), 8.4 (s, 1H, –CH=N), 6.7-9.4 (m, 7H, Ar-H), 3.82 (s, 3H, -OCH_3) ppm. ^{13}C NMR (DMSO-d_6 400 MHz) δ: 161 (C=O), 150 (C=N), 149 (C-OH), 114-150 (Ar-C), 56 (O-CH_3) ppm.

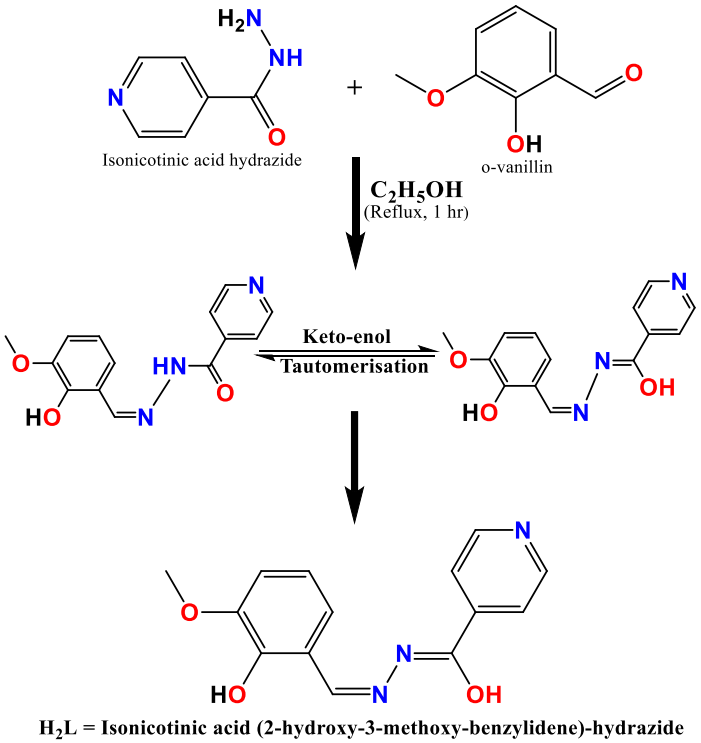

Scheme 1 Synthesis and keto-enol tautomerization of ligand **(H_2L).**

Synthesis of the dioxidovanadium(V) complexes

Synthesis of [V(O)$_2$(L)]ImH (1)

A methanolic solution (10 mL) of V_2O_5 (0.181 g, 1mmol) was added to the methanolic solution of H_2L (0.271 g, 1mmol) with stirring. To this reaction mixture (0.068 g, 1mmol) imidazole was added. The resulting reaction mixture was then refluxed for 3 hrs at 75°C, under continuous stirring, cooled to room temperature and filtered. The filtrate was left for slow evaporation after one weak, radish brown powder of **1** separated. This was filtered, washed with cold methanol and dried in a calcium chloride desiccator.

Yield: 60 %. Anal. Calc. for $C_{17}H_{16}N_5O_5V$ (421.29 g mol^{-1}). C, 48.47; H, 3.83; N, 16.62 %. Found: C, 48.46; H, 3.81; N, 16.60 %. FTIR bands (KBr, cm^{-1}): ν(C=N) 1633 (m), ν(C-O) 1291 (vs), ν(V=O) 942 (s), ν(V-O) 432, ν(V-N) 410 cm^{-1}. ESI Mass (m/z) = 422.50.

Similarly, all other complexes **2-6** were synthesized by using same procedure similar to complex **1**. The synthetic route of complexes is given in scheme 2.

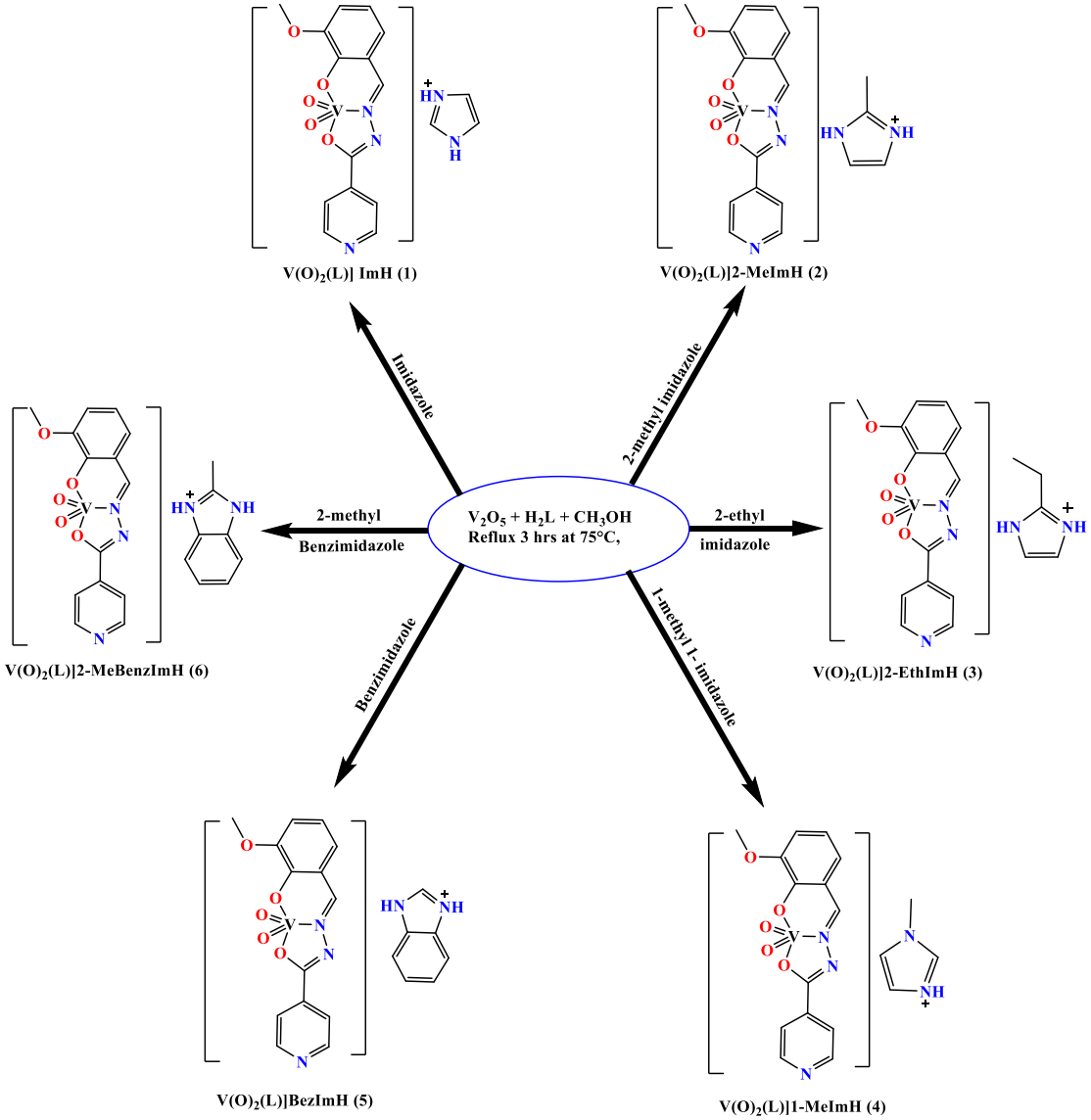

Scheme 2 Synthetic route of dioxidovanadium(V) complexes **1-6**.

NMR Spectra of Ligand

The ^{1}H and ^{13}C NMR spectra of Schiff base was measured in DMSO-d_6. The ^{1}H NMR spectrum of Schiff base shows peaks at δ = 12.2 and 10.7 ppm due to phenolic proton (s, 1H, OH) and secondary NH proton (s, 1H, NH) of isonicotinic moiety of the ligand.

Mass spectral studies

The mass spectra of complexes were in good agreement with the proposed structures. The mass of all complexes was done in positive mode only. The mass of all complexes was obtained in between the range of $[M+1]^+$ to $[M+3]^+$. The mass spectrum of **1** shows a molecular ion (m/z) peak at $[M+1]^+$ 422.50, which proves the formation of the complex. The ESI-mass of all complexes is in good agreement with the molecular mass of complexes **1-6.**

Crystal Structure of Ligand (H_2L)

The single-crystal structure displays that the enolic proton is transferred to the imine nitrogen and hence ligand is in keto-imine form. The phenolic proton forms intramolecular hydrogen bonding with imine nitrogen and thus a six-atom pocket, $R_1^1(6)$ is generated. The bond length of C1-O1 and C9-O2 have the values 1.2186(12) Å and 1.3496(11) Å respectively. Pyridine nitrogen is a bi-furcated donor atom for generating intermolecular hydrogen bonding.

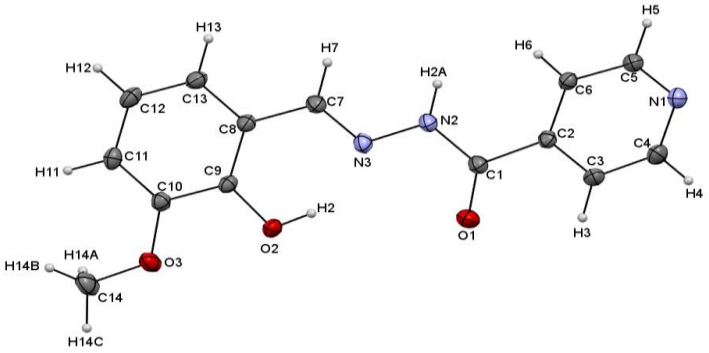

Powder X-ray diffraction

As single crystals of complexes **1-6** could not be obtained after several affords, therefore, polycrystalline X-ray diffraction patterns were collected for present complexes. However, several spectroscopic techniques could be used with good effect to characterizing these metal complexes. These complexes show peaks at 2θ = 0-80 °C exhibiting their crystalline nature. The distribution of the peaks in XRD patterns revealed an excellent crystalline for the morphology of all complexes.

Molar conductance

The molar conductance for complexes **1-6** measured in DMSO solution (1×10^{-3} M). The observed values are in 65-73 $\Omega^{-1}cm^2mol^{-1}$ range. Although these values are slightly less than the molar conductance values for a monoanionic nature (1:1:1). This could be due to the low mobility because of the large size of their ions in the solution. Therefore, these complexes show less molar conductance.

FTIR spectral study

The free hydrazone ligand shows a strong band in the 2996-3625 cm^{-1} region. This band may be assigned due to ionic contribution from ν(OH) and ν(NH) stretching. This strong band is replaced by broadband in the complexes suggesting that the phenol character of the ligand is lost. The band corresponding to ν(C=O) is absent in the IR spectrum of the hydrazone ligand. This observation supports the fact that the coordination of the hydrazone ligand to the vanadium centre in the enol form. In the free ligand band due to ν(>C=N) stretching vibration remains at 1691cm^{-1}, which shifts towards lower wave number on complexation, suggesting that the >C=N moiety is involved in bonding to the metal centre. The strong ν(V=O) stretch at ~942 cm^{-1} in all complexes is a clear indication of the dioxide nature of the complexes.

Electronic spectral studies

Electronic spectra were recorded using DMSO solutions (1.0×10^{-3} M). All complexes display similar spectral profiles. The absorption bands in the region 286-293 nm are ascribed to an intra ligand charge transfer band, while the new bands of medium intensity appear at 415-431 nm are assigned to the ligand to metal charge transfer (LMCT) band which arises from the *p*-orbital lone pair of the phenolate oxygen atom to an empty d-orbital of vanadium (V) centre. These complexes having V(V) (d^{10} system) did not show the d-d transition.

Electrochemical studies

The electrochemical behaviours of complexes **1-6** was explored using cyclic voltammetry (CV) and differential pulse voltammetry (DPV). The cyclic voltammetry complexes **1-6** have been recorded in DMSO (1.0×10^{-3} M) using 0.1 M tetra butyl ammonium perchlorate (TBAP) with Ag/AgCl as reference electrode at a scan rate of 300 mV/s at 25°C.

Hirshfeld Surface Analyses

The Molecular Hirshfeld surfaces in the crystal structure of ligand were explored based on electron distribution. A molecular Hirshfeld surface in the crystal structure was constructed based on the electron distribution calculated as the sum of spherical atom electron densities. For a given crystal structure and a set of spherical atomic densities, the Hirshfeld surface is unique. The normalized contact distance (d_{norm}) based on both d_e and d_i (where d_e is the distance from a point on the surface to the nearest nucleus outside the surface and d_i is the distance from a point on the surface to the nearest nucleus inside the surface) and the vdW radii of the atom, as given by equation 2 enables identification of the regions of particular importance to intermolecular interactions.

Molecular modelling

Optimization of the geometry of molecules is the primary step to determine the structural parameters such as bond distances and bond angles. The optimized structures are obtained using DFT studies at B3LYP/ LANL2DZ basic set level. The geometry of the vanadium(V) centre is distorted square pyramidal and distorted trigonal pyramidal. The Schiff base ligand is diatonic (L^2) with ONO donor sites. The VO_2^+ entity accommodated in the ONO binding site of tridentate ligand yields $[V(O_2)L]^-$ anion. One imidazolium ion satisfies the charge of the unit. The double bonds between V(V) dioxide oxygen atoms of 1.630-1.636 Å in distorted square pyramidal geometry are comparable to those reported in similar complexes. The fourth equatorial position is occupied by the second dioxo oxygen atom.

Frontier Molecular Orbital (FMO) analysis

The ground state electronic structures of the complexes were determined based on the optimized ground state geometry method of the synthesized complexes. The data of frontier molecules orbital (FMO) analysis were analyzed to understand the various structural features of the complexes in different viewpoints such as UV-Vis and FTIR spectra, optical properties, charge transfer, reactivity and interactions in the chemical molecule. The energy gap (ΔE_g) between the highest occupied and lowest unoccupied molecular orbitals provides information about the reactivity and nature of complexes.

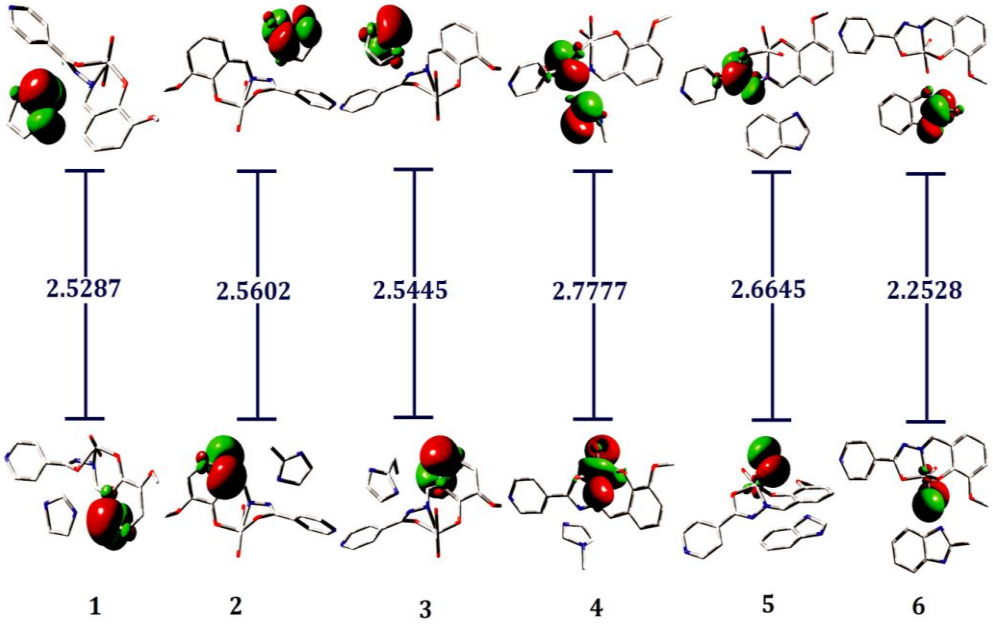

Energy profile diagram of complexes **1-6.**

Thermogravimetric analysis

Thermal analysis of the complexes was carried in an atmosphere of nitrogen at a heating rate of 10 °C /min. The thermal analysis of complexes is recorded in the temperature range of 25-650 °C**.** All complexes **1-6** are stable up to 300 °C and thereafter they decompose exothermically and showed two-step decomposition patterns.

α-Glucosidase inhibition study

The α-glucosidase inhibitory activity was assayed by using pNPG as a substrate. Shows the results of % inhibition *vs.* concentration. The major micro constituents in the biological system are carbohydrates, proteins and fats. The dominant constituents of carbohydrates are glucose, fructose, maltose and sucrose. These constituents can be easily absorbed into the blood-stream from the gastrointestinal tract. The role of α-glucosidase and α-amylase are to transform most of the polysaccharides and insoluble polysaccharides into absorbable Monosaccharides.

β-Glucosidase inhibition study

The β-glucosidase inhibition data with the substrate pNPG was also collected. The IC_{50} values for β-glucosidase inhibition activity were ranged from 200-1000 μg/mL. The inhibition

data are similar to the previously reported results. The inhibitory data showed that complex **4** exhibited the strongest inhibition and **6** showed the lowest inhibition. It is found that these complexes showed higher inhibitory activity on β-glucosidase than acarbose, which was taken as a positive control during inhibition measurements.

α-Amylase inhibition study

The α-amylase activity of complexes **1-6** were also measured. The IC_{50} and amylase activity are collected. α-amylase is involved in the inhibition of carbohydrate metabolism for the treatment of type II diabetes. Acarbose was taken as control. Acarbose is a tetrasaccharide and it inhibits *in vitro* and *in vivo* such as dextrinase, maltose, glucoamylase, sucrose and pancreatic amylase. Therefore, it is used as an inhibitor in inhibition steady of α-amylase and α-glucosidase inhibition.

Conclusions

In this work dioxidovanadium(V) complexes were synthesized using tridentate hydrazone Schiff base. The Schiff base and dioxidovanadium(V) complexes were characterized by using FTIR, NMR, single-crystal X-ray diffraction analysis, powder X-ray diffraction analysis, mass spectrometry, Hirshfeld analysis and DFT calculations. Six new dioxidovanadium(V) complexes (**1-6**) of ONO-Schiff base hydrazone has been synthesized using (H_2L**)** ligand. Due to small formed crystals, and the problem with complex recrystallization, complex decomposition, the single X-ray crystal structure could not be determined. These complexes have been characterized for their spectroscopic and redox properties. These complexes having V(V) (d^0 system) did not show a d-d transition in electronic spectra. The geometry of these complexes can be described in terms of trigonal bipyramidal or square pyramidal. Complexes **1-6** show one reductive wave and one oxidative wave. Although oxidative wave for complexes **5** and **6** are not defined. The ΔE value of **1, 3 & 4** is 465-589 mV, indicating the irreversible nature of redox waves. Besides, *in vitro* α-glucosidase, β-glucosidase inhibition activity and α-amylase inhibition activity results proved that these complexes are promising anti-diabetic agents.

Chapter 5

Syntheses, spectral characterization and antidiabetic activities of vanadium(IV/V) complexes with bi-and tridentate ligands (In situ reaction)

Synthesis of $[VO(BPA)(OH_2)_2]SO_4$ 1

Vanadyl sulphate pentahydrate (0.254 g, 1mmol) in 10 mL and 2,2'-bis(pyridylmethyl)amine (BPA) (0.1 mL, 1 mmol) in 1 mL methanol were mixed and the reaction mixture was refluxed for 3 hrs at 75 °C. A light blue precipitate was formed which was filtered, washed with methanol and dried in calcium chloride desiccator.
Yield: 65 %. Anal. Calc. (%) for $C_{12}H_{16}N_3O_3V$ (M = 397.27 g mol^{-1}): C, 36.27; H, 4.05; N, 10.57 %. Found: C, 36.23; H, 4.09; N, 10.55 %. FTIR bands (KBr, cm^{-1}): ν(C=N) 1608 vs, ν(V=O) 978 vs, ν(V-O) 483 m, ν(V-N) 430 cm^{-1}. ESI Mass (m/z) = 399.14.

Similarly complexes **2** and **3** were prepared. The synthetic route of complexes 1-3 is given in scheme 1.

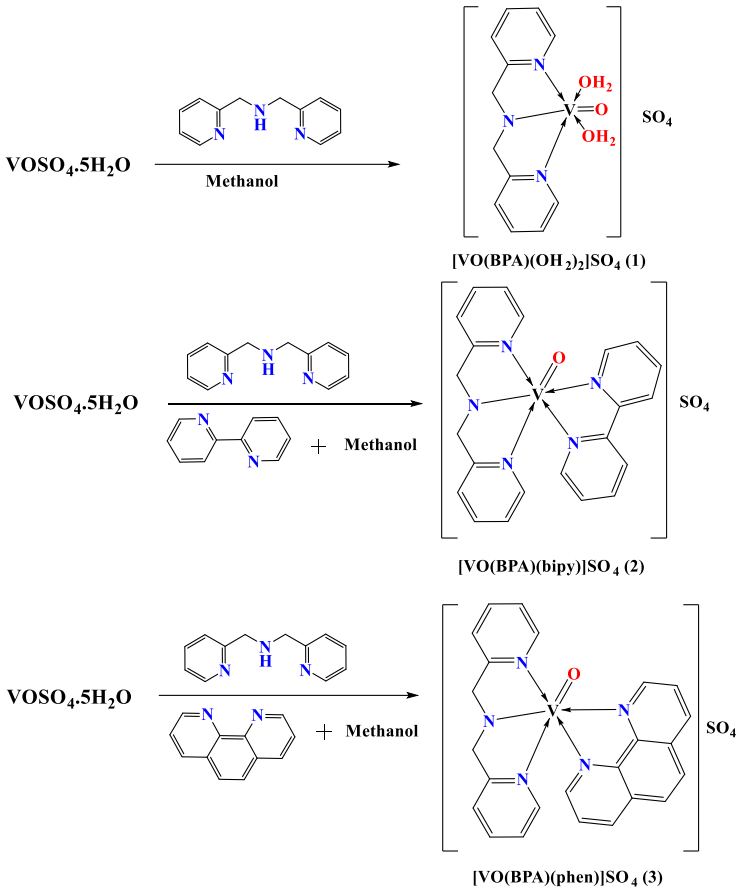

Scheme 1 Synthetic route of complexes **1-3.**

Synthesis of [VO(L^1)(Mol)] 4

To a MeOH solution (20 mL) of 5-nitrosalicylaldehyde (0.167 g, 1.00 mmol), benzhydrazide (0.136 g, 1.00 mmol) was added and the resulting solution was heated to reflux for 1 hrs at 75 °C. The reaction mixture was cooled at room temperature. To this solution, maltol (0.126g, 1.00 mmol) and $VOSO_4$ (0.163 g, 1.00 mmol) dissolved in MeOH were added. The reaction mixture was further stirred for 3 hrs to give a brown solution and allowed to evaporate slowly in the air. After one weak, dark brown product separated, this was filtered and dried in a calcium chloride desiccator.

Yield: 73 %. Anal. Calc. for $C_{20}H_{14}N_3O_8V$ (M = 475.02g mol^{-1}):C, 50.54; H, 2.97; N, 8.84 %. Found: C, 50.57; H, 2.99; N, 8.82 %. FTIR (KBr, cm^{-1}): ν(C=O) 1632 vs, ν(C=N) 1604 vs, ν(V=O) 952 vs, ν(V-O) 432 m, ν(V-N) 417 cm^{-1}. ESI Mass (m/z) = 475.73.

Similarly complexes **5-11** were prepared using same procedure as complex **4**. The synthetic route of complexes **4-11** is given in scheme 2 and 3.

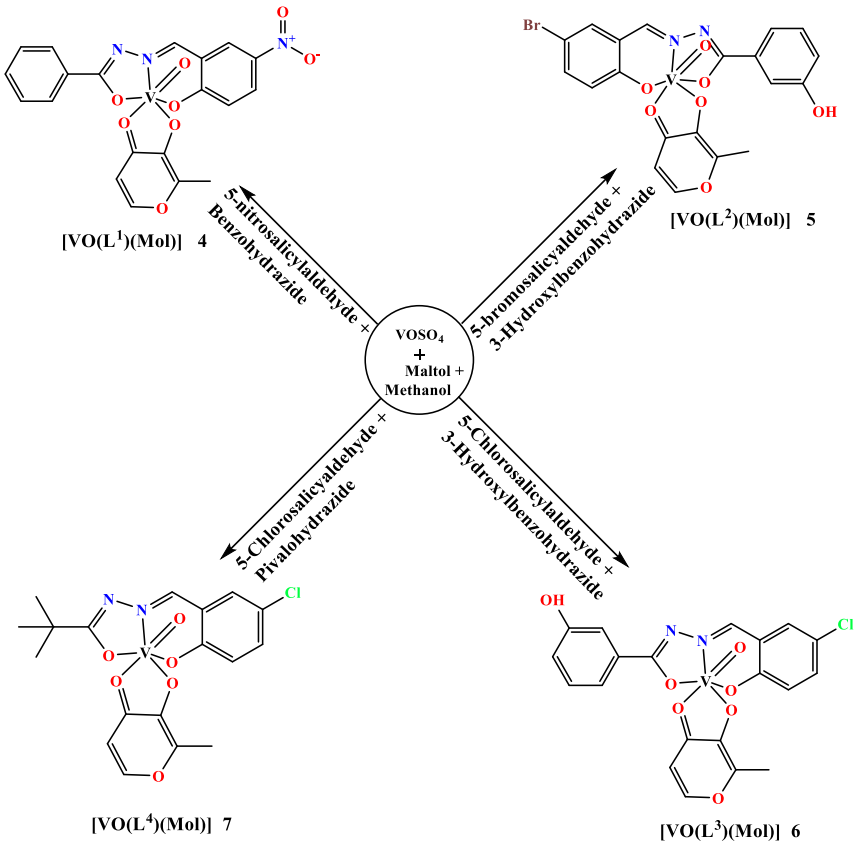

Scheme 2 Synthetic route of complexes **4-7** (with maltol).

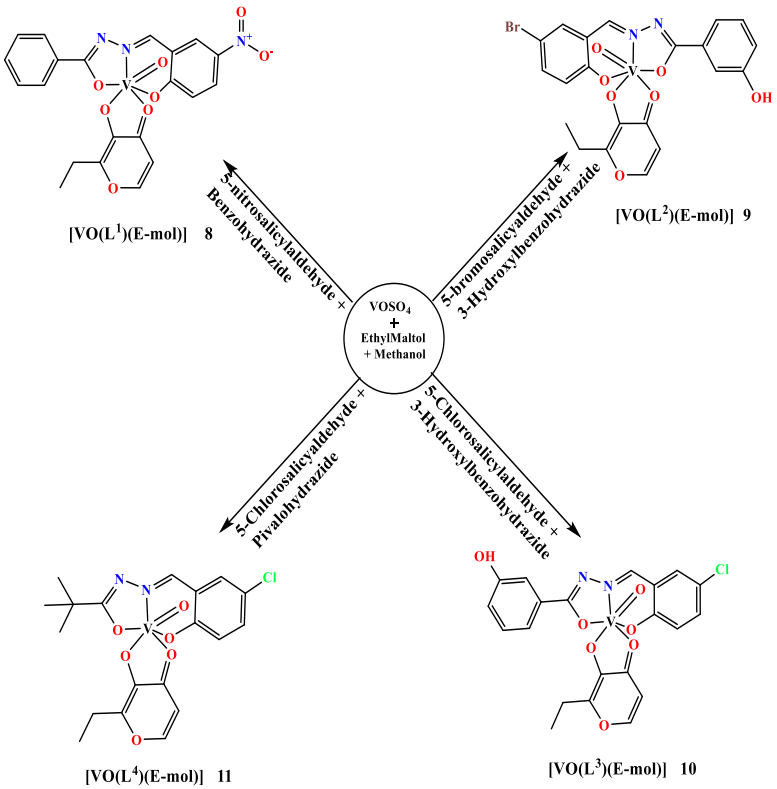

Scheme 3 Synthetic route of complexes **8-11** (with Ethyl maltol).

Powder XRD

X-ray diffractograms are used to determine the phase purity of transition metal complexes **1-3**. Diffraction was performed to obtain evidence about the structure of the metal complexes. X-ray diffractogram of complexes was scanned in the range 4-85 °C.

FTIR spectra of complexes

The FTIR spectra of complexes should some additional structural information. The FTIR spectrum of complexes **1-11** was recorded in the range of 400-4000 cm^{-1}. In FTIR spectrum of complexes **1-3,** a strong band observed in the region of 978-956 cm^{-1}, which is consistent with six-coordinated vanadium complexes. In all spectra, the band corresponding to υ(N-H) at ~ 3079 cm^{-1} is observed due to the tertiary amine moiety of BPA. The IR spectrum of complex **1** shows a band at 3434 cm^{-1}, which can be attributed to the coordinated water molecules. A new band present at 1289-1303 cm^{-1} region in the complexes assigned to the ν(C-O) (enolato) stretching mode. The absorption bands in the 1596-1606 cm^{-1} range, indicate the coordination of azomethine nitrogen to the vanadium. Moreover, the band in the regions 432-484, and 410-417 cm^{-1} can be attributed to the stretching modes of the vanadium to ligand bonds, ν(V-O) and ν(V-N), respectively.

ESI Mass Analysis

As single crystals of complexes, **1-11** could not obtain so an ESI mass of complexes was done to confirm the molecular weight of complexes. Positive mode ESI-mass of complexes were done. The ESI mass of complexes is almost similar to the calculated mass of the complexes. The mass of complexes was obtained in $[M + 1]^+$ and $[M + 2]^+$ mode.

Magnetic and EPR spectral properties

Magnetic susceptibility data of all complexes (**1-3**) were measured at room temperature. The complexes **1-3** exhibit magnetic moment 1.81, 1.79 and 1.83 BM respectively, in accord with a spin only value of vanadium complexes having VO^{2+} ion. Vanadium(IV) complexes and are quite close to the value related to these complexes.

The full range (3200–2000 G) X-band EPR spectra for the oxidovanadium(IV) complexes (frozen liquid state and room temperature solid-state) were recorded. The ESR spectra of all the complexes show a typical eight-line pattern which suggests that single vanadium is present in the molecule, i.e., it is mononuclear. The g and A-values were computed from the spectra using TCNE free radical as g marker.

Electronic spectra of complexes

UV-visible spectra of all complexes were recorded in DMSO solution (3.0×10^{-3} M). The UV-vis spectrum of all complexes has similar spectral features. The oxidovanadium(IV) complexes **1-3** exhibit bands in the range 250-500 nm, among which the two high energy bands in the UV region are attributed to the ligand centered transitions π-π* and n-π* transitions. Also, a new band of medium intensity appears in the range 450-550 nm, which is assigned to the ligand to metal charge transfer band. In the electronic spectra of complexes **4-11,** the bands in the range 300-375 nm are due to the intraligand π→π* absorption of the azomethine group. The absorption bands of 400-425 nm are assignable to n→π* of carbonyl group.

Electrochemical Study of complexes

The electrochemical behaviours of complexes (**1-3**) have been initiated using cyclic voltammetry (CV) and differential pulse voltammetry (DPV) in DMSO in the presence of 0.1 M TBAP solution. The cyclic voltammogram of **1-3** reveals a similar pattern. Only a single reduction wave at ~0.7 V is observed due to the V(IV)/V(III). The corresponding reduction wave is not observed. The cathodic peak potentials at -(0.6271-0.7085 V). The reduction process exhibits one-electron transfer i.e. the reduction of vanadium(V) to vanadium(IV). In complexes **4** and **7** one cathodic peak is due to the reduction of ligand moiety.

Thermogravimetric Analysis (TGA)

The synthesized oxidovanadium complexes **1-3** were found to be air-stable and have higher thermal stability. The thermal study was carried out using the thermogravimetric technique with a heating rate of 10 °C min^{-1}. All complexes show a two-step decomposition pattern.

α-Glucosidase inhibition activity

The pharmacologically active state of vanadium was evaluated concerning the interaction of vanadium ions and isolated rat intestinal acetone power. From these experimental results, the vanadyl state is proposed to be an active form of vanadium in enhancing insulin action by interacting with glucose carriers. It is found that the oxidovanadium complexes enhancing glucose utilization in a concentration-dependent manner over the concentration range of 100 μg/mL to 900 μg/mL.

α-Amylase Inhibition

The insulin-mimetic activity of the complexes was also estimated using the α-amylase inhibition method *in vitro*. The inhibition data exhibit that the oxidovanadium(IV) complexes stimulated glucose utilization in a concentration range of 100-900 μg/mL.

Optimized structure of complexes

Full geometry optimizations were carried out using the density functional theory (DFT) method at the B3LYP level for complex, all elements except Cu were assigned the 6-31G(d) basis se. LANL2DZ with effective core potential for Cu atom was used. The DFT optimized structure of complexes **1-11**, bond length and angle are given. The vibrational frequency calculations were performed to ensure that the optimized geometries represent the local minimum and that there is only a positive Eigenvalue. In the computational model, the cationic complex was taken into account. All calculations were performed with the GAUSSIAN 09 program.

HOMO-LUMO analysis

Interestingly, the singly occupied molecular orbital (SOMO/α-spin HOMO) is localized completely on the proligand in **4** and **6** and on tilery on metal centre in **5** and **7** in maltol (co-ligand) containing complexes except in HOMO-3. Similarly, ethyl maltol-containing complexes (**8-11**) the HOMO-LUMO energies have been estimated to find out the energetic nature and energy distribution.

Global reactivity parameters

The energies of HOMO and LUMO frontier molecular orbitals are useful in quantum chemical calculations and are related to ionization potential (IP) and electron affinity as: IP =

$-E_{HOMO}$ and EA = $-E_{LUMO}$. The other crucial chemical descriptors such as chemical potential (μ) the resistance to alternation in electron distribution are related to the stability and reactivity of a chemical moiety.

Conclusions

We have synthesized **1-11** oxidovanadium(IV/V) complexes with different ligands using in-situ process. Recent interest of inorganic, bioinorganic chemists and pharmacologists in antidiabetic oxidovanadium(IV) complexes has resulted in synthesis, characterization, and exploration of antidiabetic proportions of three new oxidovanadium(IV) complexes. All the complexes have been characterized by various physicochemical techniques. The molecular structures show the presence of six donor atoms around the oxidovanadium(IV) and hence octahedral geometry is proposed. Paramagnetic d^1 configuration of vanadium complexes (**1-3**) were supported by EPR spectroscopy. UV-Visible spectrophotometry and magnetic susceptibility measurements. These complexes were also evaluated using thermogravimetric analysis and powder X-ray diffraction techniques. The complexes show moderate *in-vitro* α-glucosidase and α-amylase inhibition. Complex **3** has an interesting insulin-like activity. Complexes **4-11** oxidovanadium(V) derived from maltol/ ethyl maltol and various tridentate aroylhydrazones were prepared and well characterized by various spectroscopic techniques. In complexes, **4-11** d-d absorption bands were not observed in all complexes being d^0 vanadium systems. The V ions in complexes **4-11** are in octahedral coordination. In complexes, the **4-11** reduction process exhibits one-electron transfer i.e. the reduction of vanadium(V) to vanadium(IV). Hence, we may conclude that these complexes may be considered antidiabetic agents.

References

1 D. Crans, S. Amin, A. Keramidas, Chemistry of relevance to vanadium in the environment. In: Nriagu, J. (Ed.), Vanadium in the Environment. Part 1: Chemistry and Biochemistry. John Wiley and Sons, New York, (1998) 73–96.

2 N.D. Chasteen, E.M. Lord, H.J. Thompson, J.K. Grady, Biochem. Biophys. Acta 884 (1986) 84-92.

3 B.R. Nechay, L.B. Naninga, P.S.E. Nechay, R.L. Post, J.J. Grantham, I.G. Macara, L.F. Kubena, D.P. Timothy, F.H. Nielson, Fed. Proc. 45 (1986) 123.

4 Y. Shechter, A. Shisheva, Endeavour 17 (1993) 27-31.

5 B.M. Lyonett, E. Martin, La Press Med. 1 (1899) 191-192.

6 K.S. Ramadan, J.M. Yousef, A.H. Hamza, S.E.Abdul Basset, Int. J. Nutr. Metab. 4 (2012) 146-150.

7 B.J. Okoli, J.S. Modise, Antioxidants. 7 (2018) 113.

8 J. Singh, R.C. Nordlie, R.A. Jorgenson, Biochimica Biophysica Acta., 678 (1981) 477-482.

9 T. Jakuscha, T. Kiss, Coord. Chem. Rev. 351 (2017)118-126.

10 S. Kumar, A. Syed, S. Andotra, R. Kaur, Vikas, S.K. Pandey, J. Mol. Struct. 1154 (2018) 165-178.

11 A.P. Tofteng, T.H. Hansen, J.Brask, J. Nielsen, P.W. Thulstrupa, K.J. Jensen, Org. Biomol. Chem. 5 (2007) 2225-2233.

12 K.H. Thomson, C. Orvig, In Metal ion in Biological systems, H. Sigel, Eds; Marcel Dekker, New York Vol. 41(2004).

13 K.H. Thompson, C. Orvig, J. Inorg. Biochem. 100 (2006) 1925-1935.

14 C. Yuan, L. Lu, Y. Wu, Z. Liu, M. Guo, S. Xing, X. Fu, M. Zhu, J. Inorg. Biochem. 104 (2010) 978-986.

15 M. Rangel, M.J. Amorim, A. Nunes, A. Leite, E. Pereira, B.de Castro, C. Sousa, Y. Yoshikawa, H. Sakurai, J. Inorg. Biochem. 103 (2009) 496-502.

16 N.R. Glover, A.S. Tracey, Biochem. 38 (1999) 5256-5271.

17 Y. Jia, L. Lu, M. Zhu, C. Yuan, S. Xing, X. Fu, Eur. J. Med. Chem. 128 (2017) 287-297.

18 E. Dogan, O. Mavis, N. Turan, H. Demir, M. Ilhan, Oriental J. Chem. 2 (2012) 57-61.

19 A. Golcu, M. Tumer, H. Demirelli, R.A. Wheatley, Inorg. Chim. Acta 358 (2005) 1785-1797.

20 F.A.E. Saied, T.A. Salem, S.A. Aly, M.M.E. Shakdofa, Pharam. Chem. J. 51 (2017) 833-842.

21 J.C. Pessoa, S. Etcheverry, D. Gambino , Coord. Chem. Rev. 301 (2014) 24-48.

22 F.A. Cotton, G. Wilkinson, C.A. Murillo, M. Bockmann, 'Advanced Inorganic Chemistry', 6th ed., Wiley Interscience, New York (1999).

23 E.M. Page, S.A. Wass, Coord. Chem. Rev. 164 (1997) 203-259.

24 E.M. Page, Coord. Chem. Rev. 172 (1998) 111-156.

25 G.J. Leigh, J.S. de Souza, Coord. Chem. Rev. 154 (1996) 71-81.

26 Q. Chen, J. Zubieta, Coord. Chem. Rev. 114 (1992) 107-167.

27 D.C. Crans, Comments Inorg. Chem. 16 (1994) 35-76.

28 D.C. Crans, J.J. Smee, E. Gaidamuskas, L. Yang, Chem. Rev. 104 (2004) 849-902.

29 A. Butler, A. H. Baldwin, Struct. Bonding, 89 (1997) 109-132.

30 D. Rehder, Coord. Chem. Rev. 181 (1999) 297-322.